Application of Ground-Penetrating Radar Methods in Determining Hydrogeologic Conditions in a Karst Area, West-Central Florida

By G.L. Barr

U.S. GEOLOGICAL SURVEY

Water-Resources Investigations Report 92–4141

Prepared in cooperation with

PINELLAS COUNTY, FLORIDA

Tallahassee, Florida
1993

U.S. DEPARTMENT OF THE INTERIOR
BRUCE BABBITT, Secretary

U.S. GEOLOGICAL SURVEY
DALLAS L. PECK, Director

For additional information, write to:

District Chief
U.S. Geological Survey
Suite 3015
227 North Bronough Street
Tallahassee, FL 32301

Copies of this report may be purchased from:

U.S. Geological Survey
Earth Science Information Center
Open-File Reports Section
Box 25286, MS 517
Denver Federal Center
Denver, CO 80225

CONTENTS

FIGURES

TABLES

Conversion Factors, Vertical Datum, Acronyms, and Additional Abbreviations

Multiply	By	To obtain
foot (ft)	0.3048	meter
foot per second (ft/s)	0.3048	meter per second
foot per nanosecond (ft/ns)	0.3048	meter per nanosecond
mile (mi)	1.609	kilometer
mile per hour (mi/h)	1.609	kilometer per hour
square mile (mi^2)	2.590	square kilometer

Sea level: In this report, "sea level" refers to the National Geodetic Vertical Datum of 1929 (NGVD of 1929)—a geodetic datum derived from a general adjustment of the first-order level nets of the United States and Canada, formerly called Sea Level Datum of 1929.

Acronyms

GPR ground-penetrating radar
NWPSTP Northwest Pinellas Sewage Treatment Plant

Additional abbreviations

MHz megahertz
µS/cm microsiemens per centimeter at 25 degrees Celsius
ns nanosecond

Application of Ground-Penetrating Radar Methods in Determining Hydrogeologic Conditions in a Karst Area, West-Central Florida

By G.L. Barr

Abstract

Ground-penetrating radar (GPR) is a useful surface geophysical method for exploring geology and subsurface features in karst settings. In GPR surveys, a radio-frequency electromagnetic signal is transmitted into the ground, and the signal reflected from subsurface lithologic and hydrologic features and boundaries can be interpreted to identify sediment thicknesses, depths to the water table and to clay beds, breaches in confining beds, karst development, buried objects, and lake-bottom structure. Data collected during GPR surveys conducted in December 1987 and March 1990 in Pinellas, Hillsborough, and Hardee Counties in west-central Florida were used to demonstrate the application of GPR methods in determining subsurface hydrogeology in a karst area.

The reflected GPR signal is principally affected by the bulk conductivity of sediments and pore fluids and the apparent dielectric constant of subsurface materials. Reflection amplitudes are a function of contrasts in apparent dielectric constants across a reflectory interface, and the apparent dielectric constant is primarily a function of water content. The effective exploration depth of a GPR survey is the maximum depth at which coherent reflections can be recognized. High subsurface conductivities attenuate the transmitted signal, limiting exploration depths. Effective exploration depths in predominantly unsaturated and saturated sand and clay sediments at the five study sites in west-central Florida ranged from a few feet to more than 50 feet below land surface. Exploration depths were limited as a result of strong signal attenuation when high conductivity clay was encountered, whereas greater exploration depths were possible when low conductivity sand was encountered.

Results of the study in west-central Florida indicate that GPR can provide information on shallow, subsurface conditions that is useful in hydrogeologic studies. Proper interpretation of the graphic record, however, depends upon the user's knowledge of the method and familiarity with the local hydrogeologic setting.

INTRODUCTION

Ground-penetrating radar (GPR) is a relatively inexpensive, nonintrusive, electrical surface geophysical method that can be used to define shallow lithologic contacts and subsurface features. Lithologic and hydrogeologic conditions that can be inferred from GPR surveys include sediment thickness, depth to the water table, breaches in confining beds, lake-bottom structure, and sinkhole development. GPR data also can be used to make lithologic or hydrogeologic correlations and to locate buried objects.

Recent technologic developments of GPR methods have lead to applications in various hydrogeologic settings. To evaluate the potential for application of GPR methods in the study area in west-central Florida, the U.S. Geological Survey, in cooperation with Pinellas County, Fla., conducted a study to demonstrate the utility of GPR methods in karst terrain. GPR surveys were made during 1987 and 1990 at five study sites in Pinellas, Hillsborough, and Hardee Counties. These sites are the Northwest Pinellas Sewage Treatment Plant (NWPSTP), the East Lake and Eldridge-Wilde well fields in northern Pinellas and northwest Hillsborough Counties, a proposed well-field site near Pemberton Creek in northeast Hillsborough County, and a phosphate-mining reclamation area on CF Industries property in northwest Hardee County (fig. 1).

Purpose and Scope

This report describes how GPR methods were used to delineate subsurface features in a karst area in west-central Florida and possible application to other hydrogeologic studies. A description of the GPR equipment used for this study, a brief overview of GPR principles, a description of the hydrogeology at five study sites, and the interpretation of GPR data collected in 1987 and 1990 at those sites are presented.

GPR data collected along approximately 11 mi of traverses at the NWPSTP site in December 1987 and along approximately 5 mi of traverses each at the East Lake, Eldridge-Wilde, and Pemberton Creek sites and about 0.3 mi of traverses at the CF Industries site in March 1990 were used to demonstrate the application of the methods. Data also were collected along 0.5 mi of traverses on a lake at the Eldridge-Wilde site in March 1990. Subsurface conditions interpreted from the GPR data collected at these sites were used in conjunction with available hydrologic and lithologic data.

Acknowledgments

The author expresses his appreciation to Pinellas County Water System personnel for providing assistance during the study. Particular thanks are extended to Daniel Christy and Arthur Finney of the Pinellas County Water System who assisted with development of the project and arranged for access to the well-field sites. Personnel of the City of Tampa and CF Industries also are gratefully acknowledged for providing access to the Pemberton Creek and CF Industries sites.

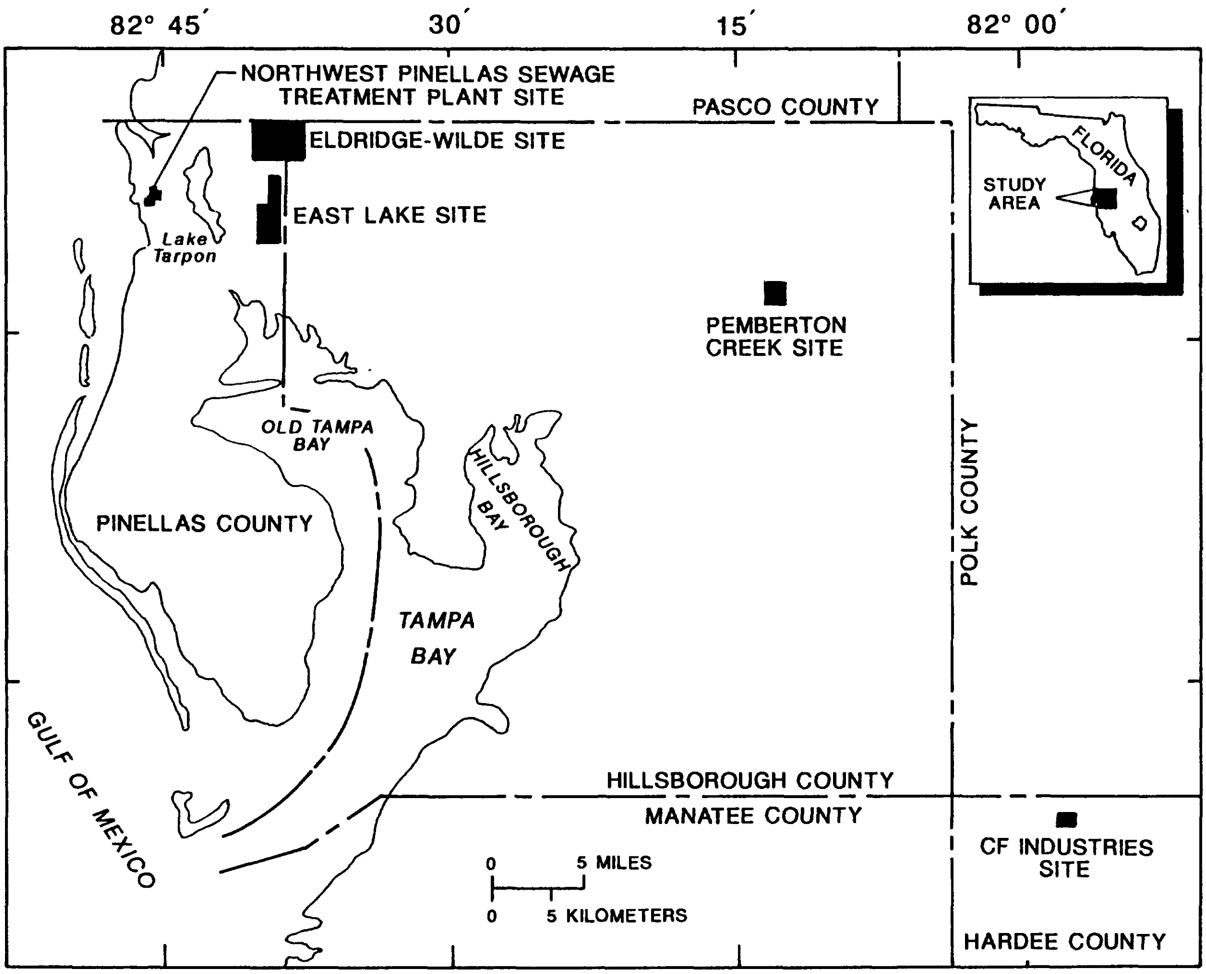

Figure 1. Locations of study sites.

Description of the Study Sites

The study was conducted at five rural sites in Pinellas, Hillsborough, and Hardee Counties. These sites are characterized by relatively flat lowlands in coastal areas and by gently rolling hills in inland areas. The NWPSTP site area, about 0.4 mi^2, is in a sinkhole plain that is typically an upland with no wetlands (U.S. Fish and Wildlife Service, 1985). Land-surface altitudes range from 5 to 50 ft above sea level. The East Lake site area, about 5 mi^2, is in a marshy, forested, scrub-shrub terrain (U.S. Fish and Wildlife Service, 1985). Land-surface altitudes range from 15 to 30 ft above sea level. The Eldridge-Wilde site area, about 5 mi^2, is in a sinkhole plain that is typically an upland with no wetlands (U.S. Fish and Wildlife Service, 1985). Land-surface altitudes range from 20 to 40 ft above sea level. The Pemberton Creek site area, about 1.2 mi^2, is in a sinkhole plain that is typically an upland with no wetlands (U.S. Fish and Wildlife Service, 1985). Land-surface altitudes range from 70 to 100 ft above sea level. The CF Industries site area, about 0.25 mi^2, is in a sinkhole plain that is typically an upland with no wetlands (U.S. Fish and Wildlife Service, 1985). Land-surface altitudes range from 116 to 130 ft above sea level.

Description of Ground-Penetrating Radar

GPR is a versatile electrical geophysical method that can be used on the land surface, on surface-water bodies, in boreholes, in aircraft, or space vehicles orbiting the earth. GPR applications can be useful for delineation of shallow hydrogeologic features. Exploration depths using GPR techniques generally range from a few feet to tens of feet, but can be greater than 100 ft in some hydrogeologic settings. The GPR equipment produces a graphic display that allows the user to interpret data while in the field. GPR equipment consists of components that are carried either manually or are towed behind vehicles or boats during a GPR traverse.

The GPR system detects the radar energy that is reflected when a pulse is transmitted through host materials. All host materials will cause some scattering and reflection of radar energy; however, greater contrasts of electrical properties at material interfaces result in stronger reflected pulses. Buried objects, such as pipes and storage containers, also commonly cause strong reflected pulses.

The principal factors that affect performance of the radar system are the electrical properties of the host material that is being penetrated by the radar energy and the transmitting frequency of the system. The ionic strength of pore fluids, degree of saturation, and porosity have the greatest effect on the electrical properties of the host material. Conductivity (or inversely, resistivity) and the dielectric constant are the principal electrical properties that affect the propagation and reflection of electromagnetic waves.

Conductivity is the measure of the ease with which current can flow through a material as a result of an applied electrical field. Resistivity, the reciprocal, is the measure of opposition to the flow of electrical current (Sheriff, 1984). Conductivity is affected by porosity, fluid properties, and the types and the quantity of clays present in the formation. Ions adsorbed by clay particles increase the conductivity of a material (Olson and Doolittle, 1985). Montmorillonite clays have a higher cation exchange capacity than kaolinite and oxide clays and, therefore, are more conductive under similar pore fluid conditions (Doolittle, 1988).

The dielectric constant is the measure of inductive capacity of a material that results from an applied electrical field (Sheriff, 1984). The dielectric constant is similar to conductivity in porous materials; it varies with the amount of pore water present (Telford and others, 1978). Materials that have higher dielectric constants (water) can store more electrical potential energy than materials that have lower dielectric constants (dry quartz sand).

General relations among conductivity and resistivity, fluid properties of host materials, the transmitting frequency, and GPR response are presented in table 1. Approximate conductivities and dielectric constants for selected materials are presented in table 2. Dielectric constants for materials at the NWPSTP site, calculated from this study, also are included in table 2. The methods used in the calculation of these values are discussed in the following sections of this report.

The conductivity and dielectric constant of a material affect the attenuation of a GPR signal (loss of radar energy), the strength of reflected radar energy, the depth of signal penetration (exploration depth), and the density of recorded traces on the graphic display. Materials with high conductivities, such as seawater and clays, greatly attenuate radar energy and cause stronger reflected pulses than materials with lower conductivities. Strongly reflected pulses are

Table 1. Effects of formation resistivity, ionic strength of formation fluid, and signal frequency on ground-penetrating radar response
[MHz, megahertz]

Higher ◄	ELECTRICAL CONDUCTIVITY of host material	► Lower
Lower ◄	ELECTRICAL RESISTIVITY of host material	► Higher
Higher ◄ (Ionic chemicals in host material: acids, bases, salts)	Ionic strength and saturation degree of fluids in host material	(Nonionic chemicals in host material: water, gasoline, hydrocarbs) ► Lower
	affects ↓	
Decreases ◄	PROBING DEPTH	► Increases
Higher ◄	ATTENUATION (loss) of radar energy	► Lower
Lower ◄	STRENGTH of reflected signal	► Increases
Thinner traces (Lighter) ◄	REFLECTION on graphic chart	► Denser traces (Darker)
Higher (1,000 MHz) ◄	FREQUENCY of transmitted pulse	► Lower (10 MHz)
	affects ↓	
Decreases ◄	PROBING DEPTH	► Increases
Increases ◄	RESOLUTION of graphic chart images	► Decreases

displayed as dense, dark traces on the graphic recorder chart. The more saturated the materials are, the greater the conductivity and attenuation of radar energy. Increased signal attenuation results in reduced exploration depth. The dielectric constant of a material affects the propagation velocity, attenuation of radar energy, and the strength of reflected radar energy, as shown by the relation in the following equations:

$$E_r = (c/V_m)^2 \qquad (1)$$

where

E_r is relative dielectric constant, dimensionless;
c is the propagation velocity in free space, in feet per second (equivalent to velocity of light, 0.98 ft/ns); and
V_m is the propagation velocity in the host material, in feet per nanosecond.

The degree of radar energy attenuation can be calculated by the equation (Morey, 1974):

$$A = 12.863\times10^{-8} f \sqrt{E_r} \left(\sqrt{\tan^2\delta + 1} - 1\right)^{1/2} \quad (2)$$

where
A is the energy attenuation, in decibels per meter;
f is the frequency, in hertz;
E_r is the relative dielectric constant, dimensionless; and
tan δ is the loss tangent.

The strength of the reflected radar energy is a function of the reflection coefficient, R, and the contrast between the dielectric constants for the two materials at the interface reflecting the signal. The reflection coefficient that is directly proportional to the strength of the reflected radar energy can be calculated by the equation (Sellman and others, 1983):

$$R = \frac{(E_{r^2})^{0.5} - (E_{r^1})^{0.5}}{(E_{r^2})^{0.5} + (E_{r^1})^{0.5}} \quad (3)$$

where
E_{r^1} is the relative dielectric constant of the upper material, dimensionless; and
E_{r^2} is the relative dielectric constant of the lower material, dimensionless.

The strength of the reflected radar energy is R^2.

The dielectric constant of a material is inversely proportional to the exploration depth (depth of penetration) of radar energy as shown in the equation

$$D = ct/2\,(E_r)^{1/2} \quad (4)$$

where
D is the exploration depth, in feet;
c is the velocity of light, 0.98 ft/ns;
t is the two-way travel time of an energy pulse, in seconds; and
E_r is the relative dielectric constant, dimensionless.

The transmitted energy is a wide-frequency pulse that lasts about 3 ns. The center frequency affects the exploration depth and spatial resolution of chart images (table 1). The frequency used is a function of balancing exploration depth against spatial resolution according to the survey objectives. The use of high-frequency short-wavelength signal pulses results in greater energy attenuation and, therefore, shallower exploration depths (eq. 2), but provides for greater resolution of the signal. The use of low-frequency, long-wavelength signal pulses increases exploration depths but reduces resolution of the signal. Because clays were present at the study sites, at depths that ranged from several feet to about 40 ft below land surface, a frequency of 80 MHz was used to provide greater penetration depths without sacrificing too much vertical resolution.

A single antenna can be used for both transmitting and receiving signal pulses in GPR surveys. Although use of a single-antenna system is commonly preferred because it is less expensive and easier to maneuver, a dual-antenna array was used for this study because it minimized unwanted surface noise and could better detect small vertical fractures in the subsurface than a single-antenna system (Benson and others, 1982).

Table 2. Conductivity and dielectric constant of selected materials

[µS/cm, microsiemens per centimeter at 25 degrees Celsius; --, no data]

Material	Conductivity (µS/cm)	Dielectric constant, E_r
Air[1]	0	1
Freshwater[1]	10^{-4} to 3×10^{-2}	81
Seawater[1]	4	81
Sand, quartz, dry[1]	10^{-7} to 10^{-3}	4 to 6
Sand, quartz, saturated (freshwater)[1]	10^{-4} to 10^{-2}	30
Silt, saturated[1]	10^{-3} to 10^{-2}	10
Clay, saturated (freshwater)[1]	10^{-1} to 1	8 to 12
Dry, sandy, flat coastal land[1]	2×10^{-3}	10
Limestone, dry[1]	10^{-9}	7
Sand and mixed soil components, dry[2]	10^{-5} to 10^{-4}	2 to 6
Mixed soil components, saturated[2]	10^{-3} to 10^{-2}	5 to 15
Quartz sand dry[3]	--	1.8 to 6.0
Quartz sand, and kaolinite, illite and smectite clays, saturated, (freshwater)[3]	--	8.9 to 67

[1]Morey, 1974.

[2]Ulriksen, 1982.

[3]Data from this study--Northwest Pinellas Sewage Treatment Plant site, Pinellas County; field-determined values from 35 sites.

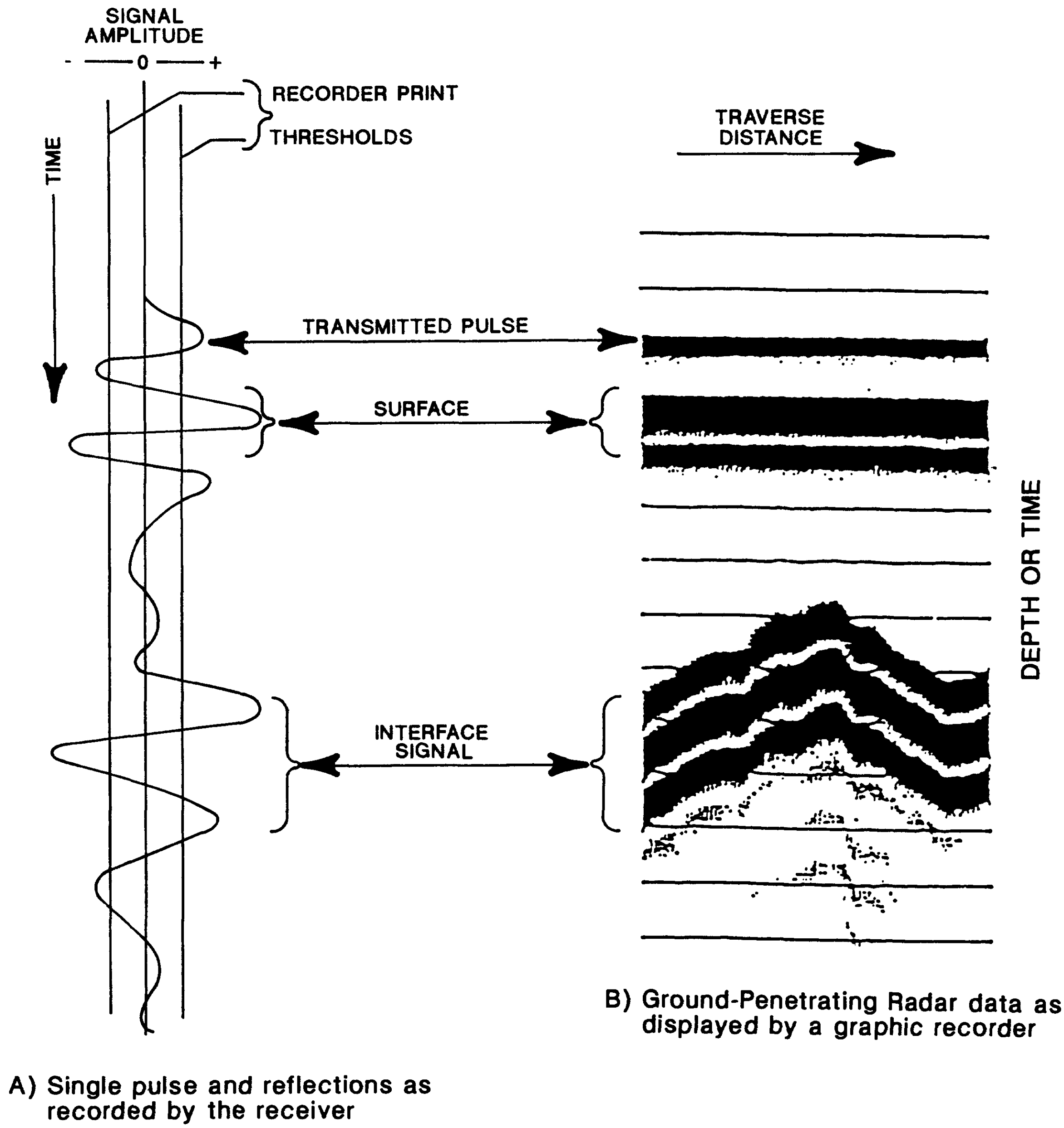

Figure 2. Simulation of a reflected pulse as recorded by the receiver and displayed by a graphic recorder. (Modified from and published with permission of Geophysical Survey Systems, Inc., 1986.)

Method of Study

Subsurface features were examined during this study by collecting GPR data along traverses across land surface and across a freshwater lake. The GPR equipment used for this study is the SIR System-8 with a dual 80-MHz antenna array manufactured by Geophysical Survey Systems, Inc. The equipment operates in the radio frequency range of 10 to 1,000 MHz by transmitting short-duration pulses of electromagnetic energy into the shallow subsurface of the terrain being surveyed. Reflected pulses are received by the antenna, processed by the system components, and displayed on a graphic recorder as a continuous time-of-travel and traverse-distance profile that is stored as data on a magnetic-tape recorder (fig. 2). Land traverses of the GPR equipment required an equipment operator in the back of a truck, a driver, and a third person to steer the antenna array. The manually guided antenna array was towed 100 ft behind the vehicle by a connecting cable.

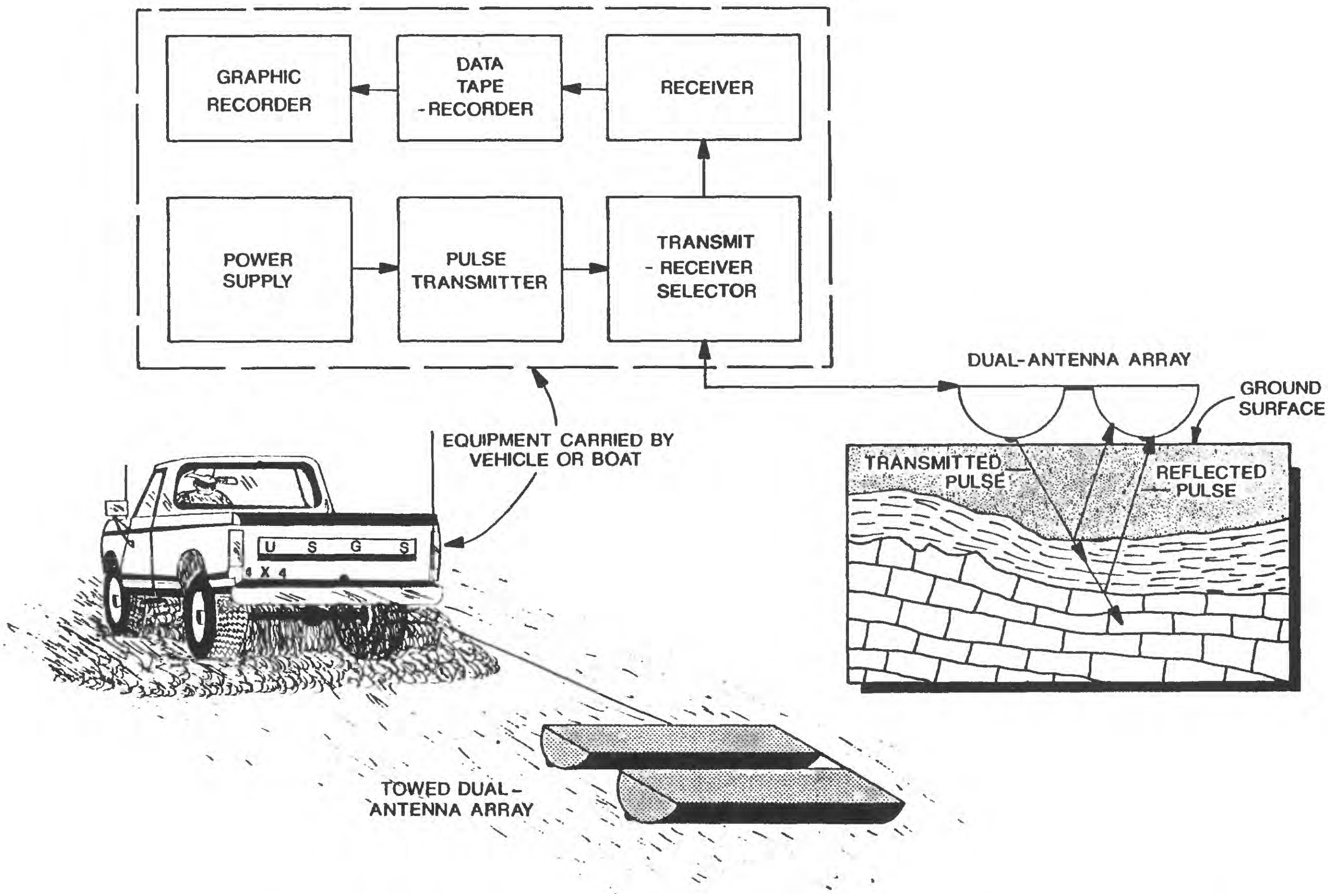

Figure 3. Functional operation of a ground-penetrating radar system used in the study. (Modified from and published with permission of Geophysical Survey Systems, Inc., 1974.)

Most traverses usually started where depth to the water table and lithology had been determined by interpreting well logs from nearby wells. The traverses continued alongside other reference wells, and the truck odometer was used to estimate the traverse distance. Reference ticks were recorded on the recorder chart at 0.1-mi intervals and additional ticks were recorded to mark other reference points, such as wells, surface features, or turns in the road. In about 2 hours, GPR data were collected along traverses totaling about 2 to 3 mi in length.

Optimum traverse speeds used for this study generally ranged between 1 and 2 mi/h. A schematic diagram that shows the functional operation of a GPR system and the land-surface application used for this study is shown in figure 3. A small boat was used for the lake traverses. The antenna array, designed to float, was towed about 50 ft behind the boat with the connecting cable supported by floats. A steel tape was used to measure the depth to the lake bottom at the start of each traverse.

HYDROGEOLOGY

This study focused on the hydrogeology of the surficial aquifer system and the intermediate aquifer system or intermediate confining unit (fig. 4) that underlie the study sites. The general regional hydrogeology consists of a thick sequence of carbonate rocks overlain by unconsolidated siliciclastic deposits that are predominantly sand and clay. Ryder (1985), Miller (1986), and Scott (1988) have described these sediments, and Scott (1988) has redefined some of the formations and included them in the Hawthorn Group of Miocene age. The formation names used in this report are based upon the geologic definitions of Scott (1988) and are the accepted usage of the Florida Geological Survey.

Sedimentary units of Oligocene to middle Miocene age that include the Suwannee Limestone and the Arcadia and lower Peace River Formations of the Hawthorn Group are predominantly fossiliferous limestone and dolomite. This sequence contains appreciable amounts of siliciclastic materials with varying amounts of phosphorite. Layered sediments of upper Miocene to Holocene age that include the upper Hawthorn Group and younger sediments are predominantly fine-grained quartz sand and clay containing varying amounts of carbonate and phosphate. Smectite and palygorskite are the dominant clay minerals in the Peace River Formation; however, where carbonate rocks are dominant, smectites and palygorskites occur only in the lower part of the Peace River Formation (Scott, 1988).

The surficial aquifer system, the intermediate aquifer system or intermediate confining unit, and the Upper Floridan aquifer are the major hydrogeologic units at the five study sites (fig. 4). The locations of hydrogeologic sections at each study site are shown in figure 5, and the generalized hydrogeologic sections are shown in figure 6. These sections depict the thicknesses and altitudes of the units that underlie the study sites. These hydrogeologic settings generally are typical for central Florida.

Surficial Aquifer System

The surficial aquifer system in sediments of Pliocene to Holocene age is unconfined and is composed of fine to medium-grained quartz sand with clay, silt, and phosphorite (table 3). Thickness of the surficial aquifer system ranges from 5 to about 50 ft at the NWPSTP site (J.T. Trommer, U.S. Geological Survey, written commun., 1991), from 5 to 67 ft at the East Lake and Eldridge-Wilde sites, from 12 to 43 ft at the Pemberton Creek site, and from 15 to 30 ft in unmined parts of the CF Industries site (fig. 5). Depth to the water table varies with seasonal rainfall. The water table is at its highest level during the rainy

System	Series	Stratigraphic unit		Major lithologic unit	Hydrogeologic unit
Quaternary	Holocene and Pleistocene	Surficial sand, terrace sand, and phosphorite		Sand	Surficial aquifer system
Tertiary	Pliocene	Undifferentiated deposits		Sand, clay, and limestone	Intermediate aquifer system or confining unit where aquifer is absent
	Miocene	Hawthorn Group	Peace River Formation		
			Arcadia Formation		Upper Floridan aquifer
			Tampa Member	Limestone and dolomite	
	Oligocene	Suwannee Limestone			

Figure 4. Generalized correlation chart for stratigraphic and hydrogeologic units at the study sites. (Modified from Ryder, 1985; Scott, 1988.)

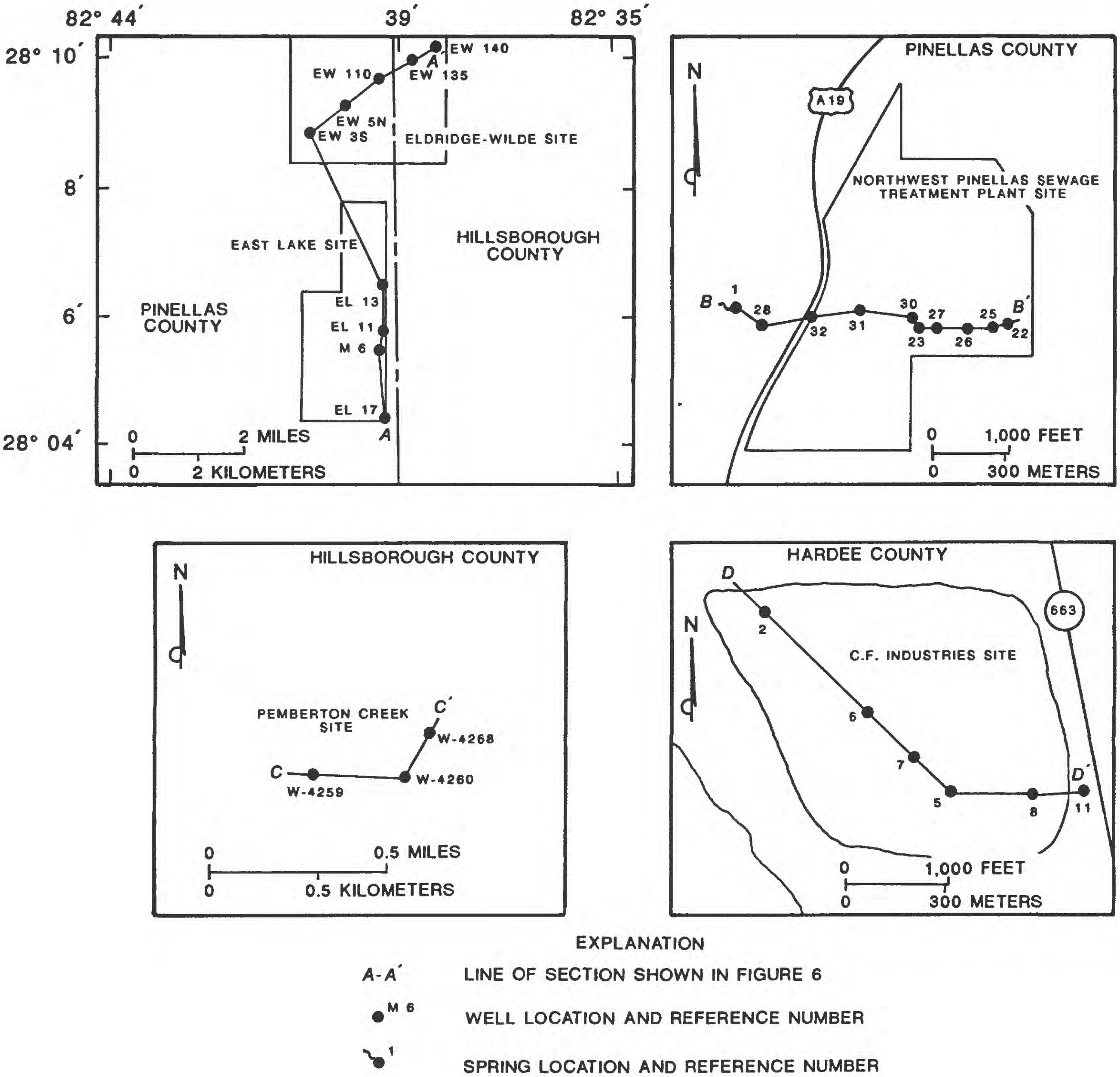

Figure 5. Locations of hydrogeologic sections.

season (June through September) and declines to its lowest level at the end of the dry season in May. The water table ranges from near land surface to about 32 ft below land surface at the NWPSTP site, from near land surface to about 20 ft below land surface at the East Lake and Eldridge-Wilde sites, from near land surface to about 6 ft below land surface at the Pemberton Creek site, and about 1 to 3 ft below land surface at the CF Industries site.

Intermediate Aquifer System or Intermediate Confining Unit

The intermediate aquifer system occurs in the study area as a Miocene to Pliocene age sequence of permeable carbonate rocks and low permeability sand, silt, and clay that underlie the surficial aquifer system. Where the system is composed only of low permeability sediments, it is the “intermediate confining unit”

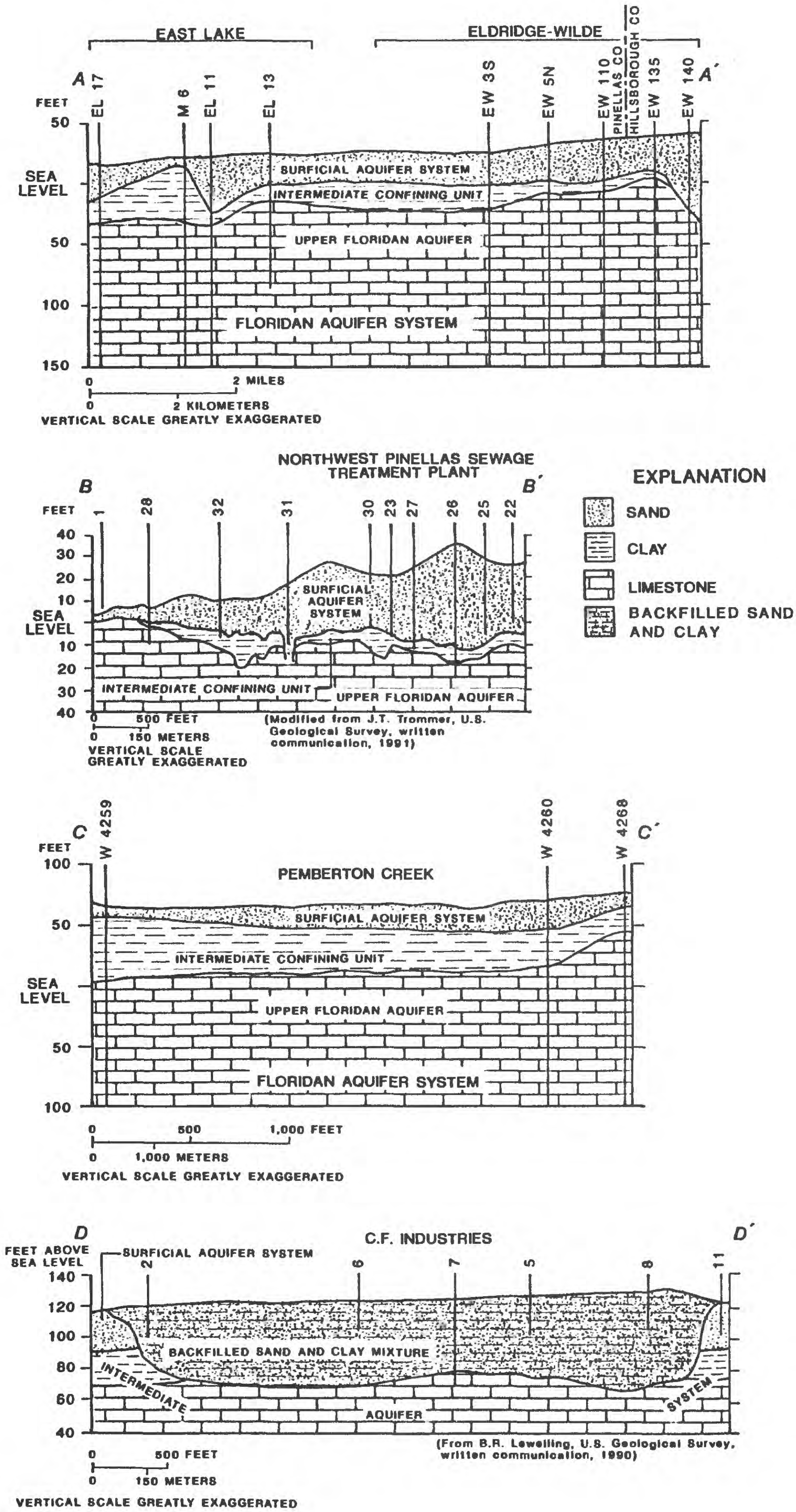

Figure 6. Generalized hydrogeologic sections.

Table 3. Radar-pulse velocity in selected materials and minimum and maximum depths of subsurface features at selected study sites

[Velocities were calculated by using equation 1 and dielectric constants in table 2; exploration depths were calculated by using root mean square velocities with equation 5; ft/ns, feet per nanosecond; ft, feet; --, no data]

Material	Radar-pulse velocity, V_m (ft/ns)	Minimum and maximum depth of subsurface features (ft)
Air[1]	0.98	--
Freshwater[1]	0.11	--
Seawater[1]	0.11	--
Sand, dry[1]	0.40 to 0.49	
Sand, saturated (freshwater)[1]	0.18	--
Silt, saturated[1]	0.31	--
Clay, saturated (freshwater)[1]	0.28 to 0.35	--
Dry, sandy, flat coastal land[1]	0.31	--
Limestone, dry[1]	0.37	--
Sand and mixed soil components, dry[2]	0.40 to 0.69	--
Mixed soil components, saturated[2]	0.25 to 0.44	--
Quartz sand, dry[3]	0.40 to 0.73	[4]6.7 to 35.8
Quartz sand, and kaolinite, illite and smectite clays, saturated, (freshwater)[3]	0.12 to 0.33	[5]2.8 to 24.6 [4]7.5 to 53

[1]Morey, 1974.

[2]Ulriksen, 1982.

[3]Northwest Pinellas Sewage Treatment Plant site, Pinellas County; field-determined values from 35 sites.

[4]Below land surface.

[5]Below water table.

(Southeastern Geological Society, 1986). The intermediate aquifer system is not present at the Pinellas County and Hillsborough County study sites, but is present in Hardee County at the CF Industries site where it averages 400 ft in thickness (Duerr and others, 1988).

The intermediate confining unit generally is present at the Pinellas and Hillsborough County study sites; however, in some places, the low-permeability sediments are thin or have been completely eroded (Scott, 1988). The intermediate confining unit at the Pinellas and Hillsborough County study sites consists of unconsolidated clays, silts, and sands with varying amounts of phosphorite (Scott, 1988). Thickness of the intermediate confining unit ranges from 0 to about 15 ft at the NWPSTP site, from about 5 to 45 ft at the East Lake site, from 0 to about 25 ft at the Eldridge-Wilde site, and from about 25 to 62 ft at the Pemberton Creek site (fig. 5).

Upper Floridan Aquifer

The Upper Floridan aquifer in sediments of Tertiary age is the upper hydrogeologic unit of the Floridan aquifer system. The top of the Floridan aquifer system is the top of a vertical section of permeable carbonate rocks that are hydraulically connected and whose permeabilities are several orders of magnitude greater than that of the overlying rocks (Miller, 1986).

The uppermost part of the Upper Floridan aquifer is the Tampa Member of the Hawthorn Group at the East Lake, Eldridge-Wilde, CF Industries, and NWPSTP sites and the Peace River Formation of the Hawthorn Group at the Pemberton Creek site (fig. 4). Limestone and dolomite are the dominant constituents of this fossiliferous, sandy, and in some places, clayey and phosphatic stratigraphic unit. The Upper Floridan aquifer at the Pinellas County and Hillsborough County study sites is at shallow depths, ranging from less than 5 ft to more than 70 ft below land surface and averaging 50 ft below land surface (fig. 5). Well completion reports from the Florida Department of Environmental Regulation indicate that the Upper Floridan aquifer is about 250 ft below land surface at the CF Industries site in Hardee County.

INTERPRETATION OF GROUND-PENETRATING RADAR DATA

Knowledge of the local lithologic conditions, equipment settings, transmitting frequency, and antenna array response to the effects of exploration depth and graphic resolution is required to interpret GPR data. Interpretation of GPR data can be simple if stratigraphy is uniform and there are sharp contrasts in electrical properties at reflective surfaces. Interpretation of GPR data is more complicated, however, when litho-stratigraphic conditions are complex or when sediments with gradual changes of electrical properties provide weak contrasts in the recorded data. Detailed equipment settings are not discussed in this report, but are described within the operating manuals of the various GPR systems (Geophysical Survey Systems, Inc., 1974).

An important aspect of interpreting GPR data is understanding the graphic display on a recorder chart or computer display. After the reflected signal pulses are received by the GPR system, they are processed into usable data and are displayed by a graphic recorder, as shown by the simulation in figure 2 and the graphic-recorder chart in figure 7. The graphic-recorder chart shows reflective surfaces and subsurface features in shades of gray to black. Graphic-recorder settings can change the contrast and shading on the chart to enhance or deemphasize selected subsurface features. Scales are used to show the horizontal traverse distance of the GPR equipment and the two-way travel time of the reflected pulse. Dark bands at the top of the chart represent components of the pulse through the air between the dual array antenna (see fig. 3) and reflected pulses from the land surface and antenna housing (fig. 7). The bands at the top of the chart often are indiscernible from each other. Subsurface features or reflective surfaces will be displayed lower on the chart as groups of dark multiple-reflection bands. Groups of two or three dark bands, rather than a single band, are characteristic of the SIR System-8 because of oscillations of the reflected signal pulse. Individual dark band groups will be superimposed if sediment interfaces are closely spaced, thus limiting the ability to distinguish between the interfaces as displayed on the chart.

Operating GPR equipment over surface-water bodies may cause multiple reflection patterns on the graphic display as a result of radar energy that reverberates between the bottom surface and the air-water surface. Multiple reflections have been reported by other investigators (Beres and Haeni, 1991) when using GPR equipment over surface-water bodies. Multiple reflections generally are not seen in applications over land surfaces.

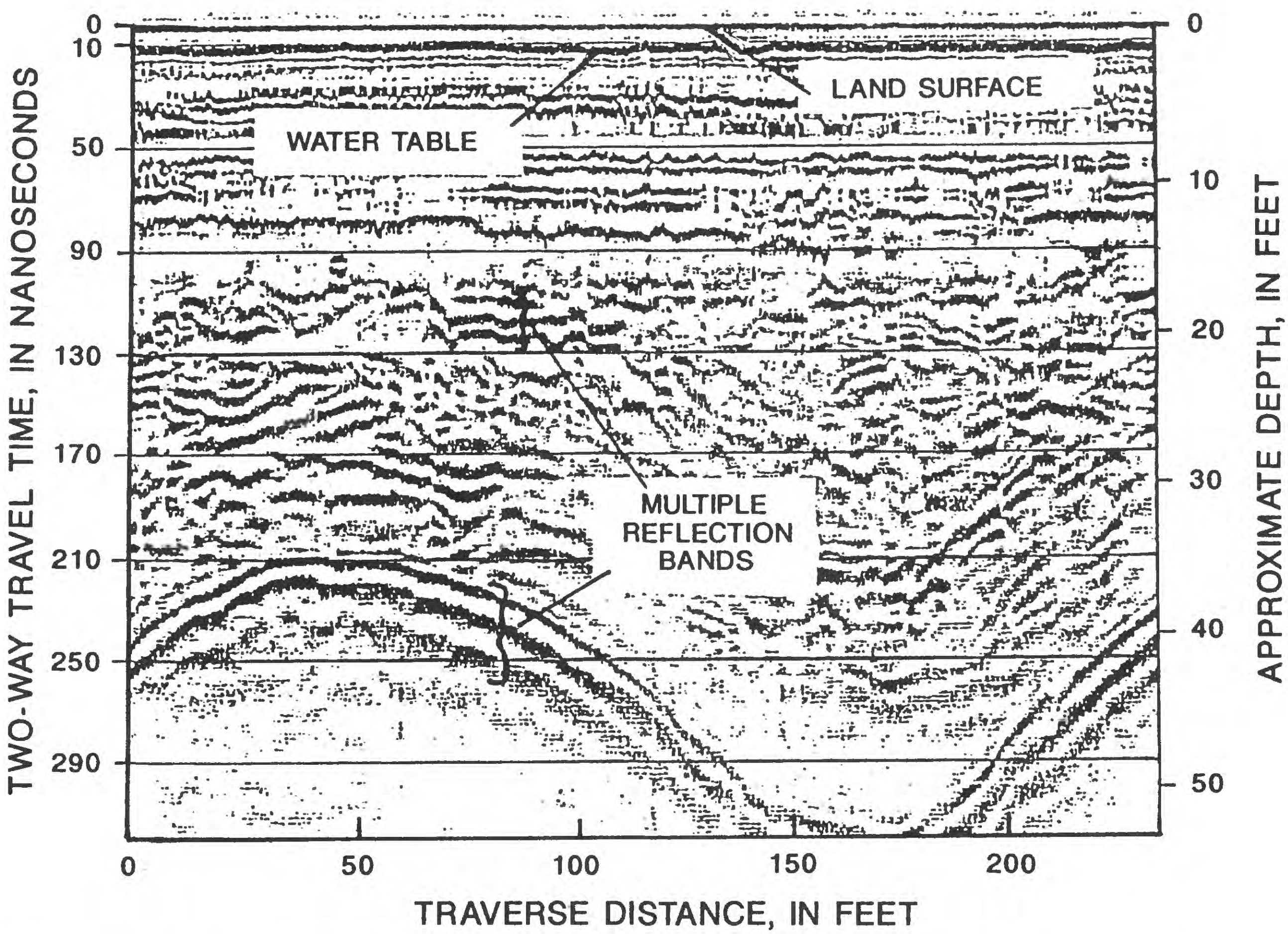

Figure 7. Graphic-recorder chart of ground-penetrating radar profile features and reflection components.

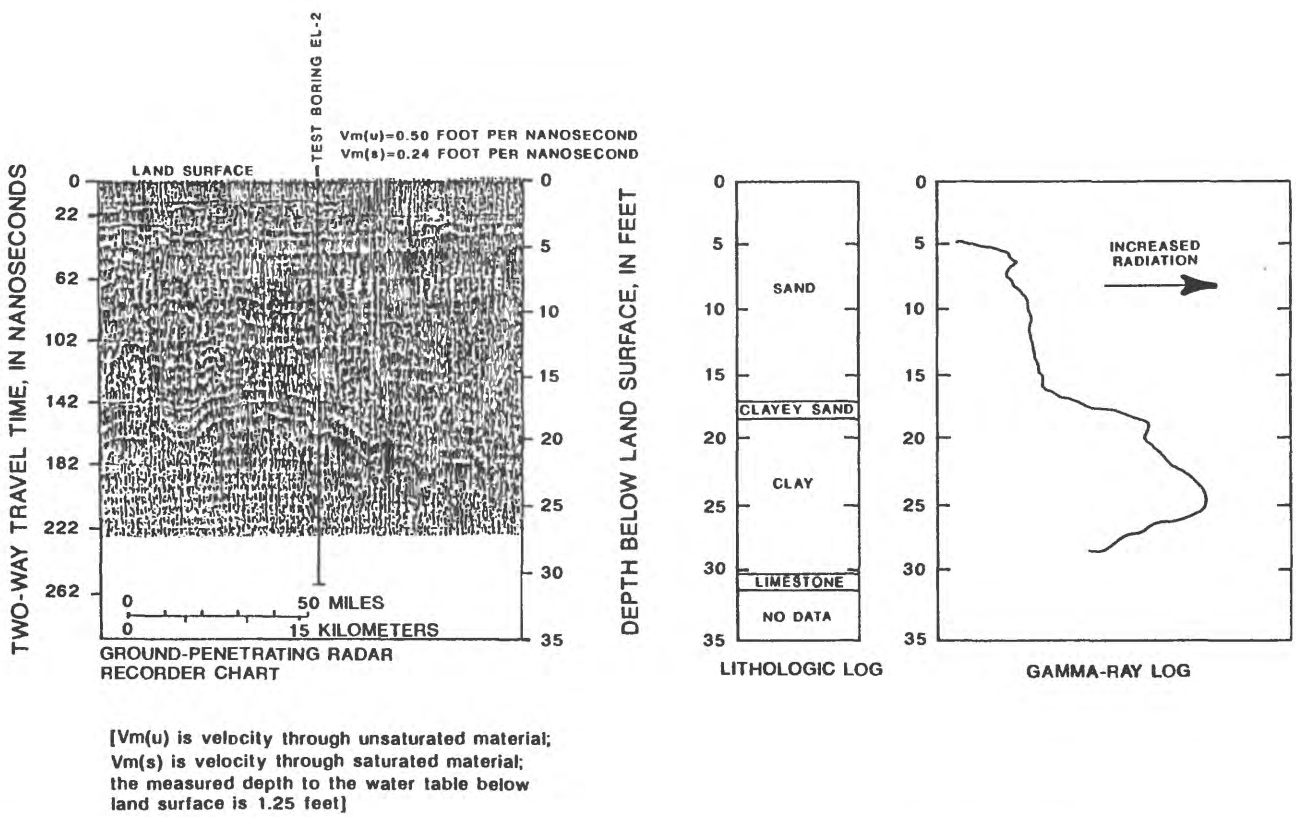

Figure 8. Ground-penetrating radar data and lithologic and gamma-ray logs at the Eldridge-Wilde site.

Interpretation of GPR data may be complicated because of interference or noise from various sources. Faulty equipment cables or placement of the antenna array too close to the towing vehicle can result in signal noise. Interference sources, which may be difficult to eliminate, include reflections from overhanging trees or power lines when using unshielded antennas, reflections from metal surface debris or fences, and electromagnetic noise from high-tension power lines or radio transmissions. When possible, a traverse should be located where such sources of interference are minimized or eliminated. Noise in the radar signal can be reduced by adding electronic filter circuitry to the GPR equipment or by adjusting the graphic recorder to achieve an optimum display when collecting field data. Processing the radar signal by the use of a computer can enhance or deemphasize GPR profile features, remove signal noise, and eliminate multiple reflection bands.

The depth of a subsurface feature or reflector can be estimated if the propagation velocity of a radar pulse is known. The relation between propagation velocity and depth is expressed by the equation

$$V_m = 2D/t \qquad (5)$$

where

V_m is the propagation velocity, in feet per nanosecond;
D is the depth to subsurface feature, in feet; and
t is the two-way travel time, in nanoseconds.

Depth to a subsurface feature, therefore, can be calculated by rearranging equation 5 to

$$D = V_m t/2. \qquad (6)$$

If the relative dielectric constant is known, then the depth to a subsurface feature also can be calculated by using equation 4.

Assumptions about depths of subsurface features need to be verified along several points of the GPR traverse by calibrating the GPR data with other field observations. Subsurface properties may be obtained by drilling test borings to obtain lithologic descriptions, geophysical logging, or measurements of the water table. A GPR recorder chart with lithologic and gamma-ray logs for the Eldridge-Wilde site is shown in figure 8. The darker reflection on the recorder chart at test boring EL-2 at a two-way travel time of about 142 ns probably represents the interface between the top of the clay bed and the overlying sediments. Clays in west-central Florida commonly contain phosphate or potassium, sources of gamma radiation, that cause "kicks" (sudden deflection of the trace) on borehole gamma-ray logs. The kick on the gamma-ray log in figure 9 that coincides with the top of the clay on the lithologic log at about 18 ft below land surface indicates that the reflection on the GPR recorder chart coincides with the top of the clay bed. The lithologic and gamma logs are used for calibration and to provide supporting evidence that the reflection is the top of the clay bed. The calculated propagation velocities through the unsaturated and saturated materials seem to be correct based on these data.

The velocity and the relative dielectric constant are often unknown. In this situation, the depth to a subsurface feature, such as the water table or a sediment layer, is determined with other field observations. This depth measurement can be used in equation 5 to calculate a velocity for a specific material. The calculated velocity can then be substituted into equation 6 to estimate depths to reflectors in other areas, but this velocity is an average and should be applied to other reflectors with caution. The velocity decreases when the radar pulse penetrates below the water table, and two velocities are needed to determine depths: one for unsaturated material and one for saturated material.

To help calibrate the depth of specific subsurface features on a recorder chart, the GPR equipment is passed by reference wells where the depths of the water table and specific lithologic features are known. An example of this procedure is shown in figure 9 using a profile from the NWPSTP site. The depth of the water table at well 1943, as measured by steel tape, is 24.04 ft below land surface. Values from the recorder chart are substituted into equation 5 to verify that the subsurface feature at 78.75 ns on the chart record is the water table, as shown below;

$V_m = 2D/t$

$V_m = 2(24.04 \text{ ft})/78.75 \text{ ns}$

$V_m = 0.61$ ft/ns, apparent propagation velocity.

Because the propagation velocity through dry sand (0.61 ft/ns) is within the velocity range for similar materials (table 3), the reflection at 78.75 ns is assumed to be the water table; the water was 1.05 in. below land surface on the original recorder chart, as shown in figure 9. The depth of the water table at reference well CLU #3, as measured by steel tape, is 32.80 ft below land surface. The depth of the water table at reference well 1951, as measured by steel tape, is 22.02 ft below land surface. Apparent velocities are calculated by using equation 5 to verify the depth of the water table at wells CLU #3 and 1951:

$V_m = 2D/t$

$V_m = 2(32.80 \text{ ft})/111 \text{ ns}$

$V_m = 0.59$ ft/ns, apparent propagation velocity at well CLU #3; and

$V_m = 2(22.02 \text{ ft})/72.75 \text{ ns}$

$V_m = 0.61$ ft/ns, apparent propagation velocity at well 1951.

The apparent velocities in the unsaturated zone at reference wells CLU #3 and 1951 also are within the expected range (table 3). Assumptions can be made for depth of the water table along the traverse at any point by using equation 6 and substituting an average propagation velocity of 0.61 ft/ns and two-way travel times derived from the recorder chart and the chart scale.

Under saturated conditions, propagation velocities below the water table are calculated by the same steps as those used for unsaturated conditions. The lithologic log for well 1943 indicates a clay bed at about 13.50 ft below the water table. To test whether the new reflector (at 101.25 ns on the chart in fig. 9) is the clay bed, substitution of these values into equation 5 yields

$V_m = 2D/t$

$V_m = 2(13.46 \text{ ft})/101.25 \text{ ns}$

$V_m = 0.27$ ft/ns, apparent propagation velocity.

The apparent propagation velocity is assumed to be correct because it is within the range (0.12-0.33 ft/ns) for similar saturated materials (table 3). Propagation velocities through saturated material also were calculated for wells CLU #3 and 1951. These velocities also were within the expected range and the reflector probably is the top of the clay bed. The assumption that the top of the clay bed at well 1943 is the subsurface feature on the recorder chart is substantiated by an expected propagation velocity and direct knowledge of the subsurface lithology. Data from lithologic and geophysical logs at several wells are needed for correlation purposes to aid in the hydrogeologic interpretation of the GPR record shown in figure 9.

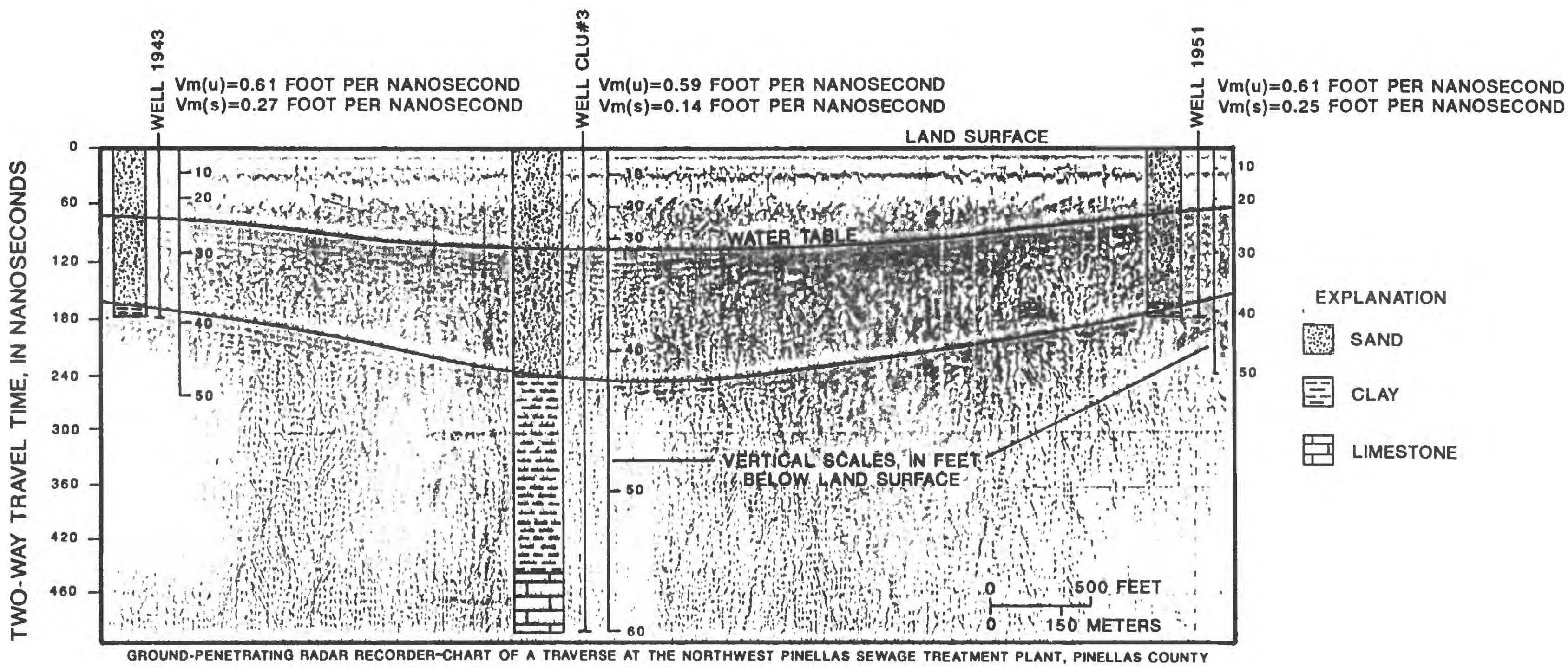

Unsaturated zone

Well	Depth of water table, in feet (field measured with steel tape)	Distance on original recorder chart from land surface to water table, in inches	Chart scale, in nanoseconds per inch (ground-penetrating radar equipment setting)	Two-way travel time[1], in nanoseconds
1943	24.04	1.05	75	78.75
CLU#3	32.80	1.48	75	111
1951	22.02	.97	75	72.75

Saturated zone

Well	Depth of new reflector below water table, in feet (derived from lithologic log)	Distance on original recorder chart from water table to new reflector, in inches	Chart scale, in nanoseconds per inch (ground-penetrating radar equipment setting)	Two-way travel time[1], in nanoseconds
1943	13.50	1.35	75	101.25
CLU#3	10.20	2.0	75	150
1951	12.50	1.35	75	101.25

[1]Product of distance on recorder chart from water table to new reflector and chart scale.

Figure 9. Ground-penetrating radar profile with depth determinations of subsurface features.

Minimum and maximum depths of subsurface features detected using GPR techniques for selected materials at selected study sites are presented in table 3. The radar-pulse velocities and depths of reflectors were determined from calculations at 35 well locations at the Pinellas County site. The dry material at the sites was quartz sand, and the saturated material consisted of quartz sand overlying clays.

Types of materials in the subsurface cannot be directly identified by use of GPR; however, reflector geometrics and characters on the radar graphic display can be useful for identification. Beres and Haeni (1991) classified the various types of reflection configurations according to lithostratigraphic features in a GPR study of stratified drift deposits in Connecticut. Seismic reflection interpretation methods were extended to GPR technology by relating layered, reflection-free, and chaotic reflection configurations to various sediment textures and grain sizes. All reflectors in GPR charts are depicted referenced to a flat antenna traverse surface on the graphic display. The geometry of the subsurface interfaces will appear as they are in the GPR graphic display if the antenna traverses over a relatively flat surface. Because all GPR traverses are not over flat terrain, changes in surface altitude result in distortions of subsurface features. For example, when traversing up a hill where the water table is at a constant altitude, the land surface will appear to be flat on the graph, and the water table will appear as a dipping feature with increasing depth in the direction of the traverse. Therefore, for data collected in the field, corrections for surface relief should be made to restore reflection features to their normal geometry. Land-surface altitude data can be used to remove the effects of surface relief if the GPR data collected are digitally recorded. The GPR profiles used in this report are uncorrected for surface relief because the distortion of subsurface features was not considered critical to demonstrate GPR techniques at the study sites.

Assuming relatively flat topography and sediments that are uniform or arranged in horizontal layers, interfaces between sand and clay and unsaturated and saturated material are depicted on a GPR graphic display as horizontal or gently sloping features. Figure 9 shows a GPR profile with interpretation of subsurface linear features. The water table and the interface between sand and clay materials shown on the GPR profile have been verified by field-test observations of water levels and by lithologic descriptions of well cuttings or samples from test-hole borings. Overhead power-lines, trees, buried objects, and sediment features, such as cavities, hard nodules, and pinnacles of consolidated sediments or rock, are point reflectors and appear on the profile as inverted V's or chevron-shaped traces (fig. 10-13). Figure 10 shows a buried polyvinylchloride (PVC) irrigation pipe, and figure 11 shows a buried concrete culvert pipe. A feature tentatively identified as a cavity below a sinkhole is shown on figure 12. This feature was not verified, but the area has many sinkholes, and other investigators have documented some chevron shapes as cavities (Ballard, 1983; Benson and others, 1982). Some chevron shapes are a reflection from curved features or objects (Ballard, 1983). The flattened chevron shape shown in figure 13, for example, can be interpreted as a pinnacle of consolidated sand.

Interfaces between the materials indicated on the GPR display become complex and may appear contorted or chaotic when sediments have been disturbed. Some disturbed sediments are the result of geologic processes, such as karst development, or are due to the direct influence of man. As indicated by the interpreted GPR profiles in figures 14 through 16, karst development has affected the shallow, unconsolidated sediments in west-central Florida. Figure 14 shows a GPR traverse at the Pemberton Creek site. Lithologic data from wells at the study site indicate the sand averaged about 20 ft thick, but sand was encountered to a depth of more than 150 ft at well 17. The interpreted GPR profile indicates sinkhole development. The sediments within the interpreted sinkholes in figure 15 have chaotic reflection patterns that are characteristic of disturbed or deformed sediments. Figure 16 shows a GPR profile through a stand of cypress trees within a sinkhole, called a cypress dome, at the Eldridge-Wilde site where sinkhole development has resulted in bowl-shaped topography. A test boring more than 50 ft deep in the bowl-shaped area penetrated sandy, silty peat and peaty sands and silts.

Disturbed sediments also may exhibit sharp contrasts on the GPR profile. For example, figure 17 shows a GPR profile over an area mined for phosphate ore. The land was reclaimed by filling the mined area with a watery mixture of sand and clay that settled into relatively flat layers. The features on the left side of figure 17 indicate the mined and reclaimed area; contrasting features on the right side show unmined sediments. The features on the left side of figure 17 fade with increasing depth because the radar energy was attenuated by the clay in the mixture that was used to backfill the mined area.

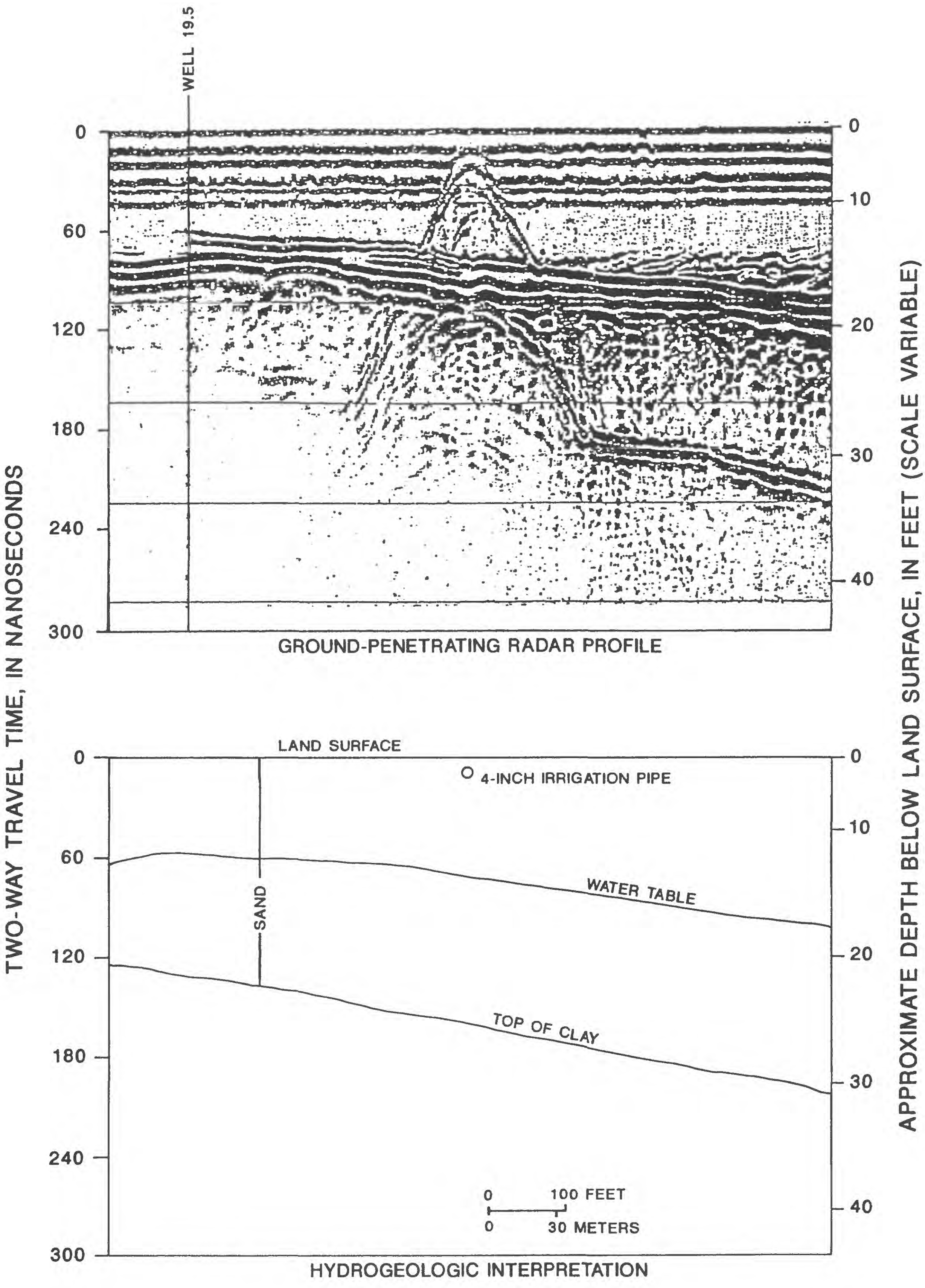

Figure 10. Ground-penetrating radar profile and hydrogeologic interpretation along a traverse over a buried polyvinylchloride irrigation pipe.

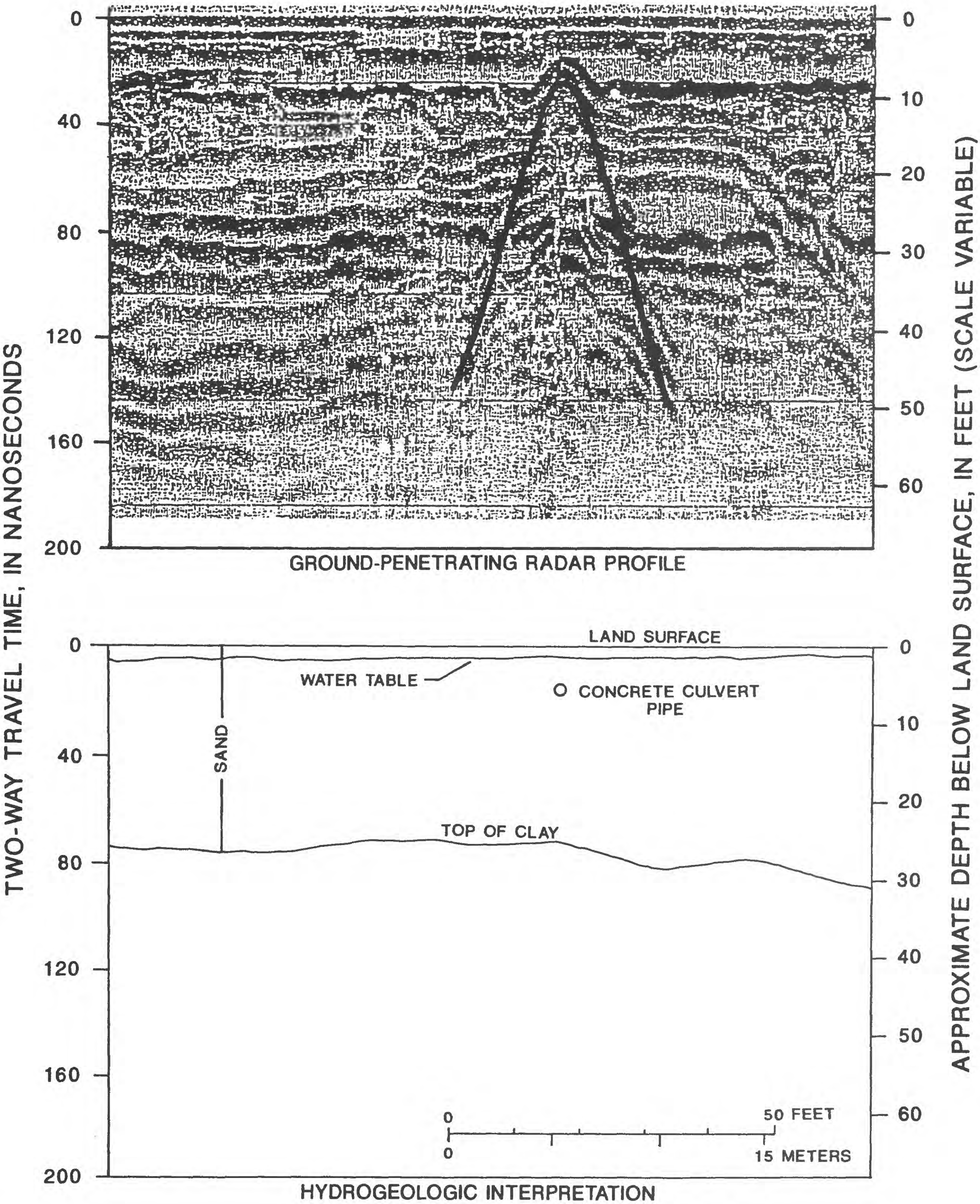

Figure 11. Ground-penetrating radar profile and hydrogeologic interpretation along a traverse over a buried concrete culvert pipe.

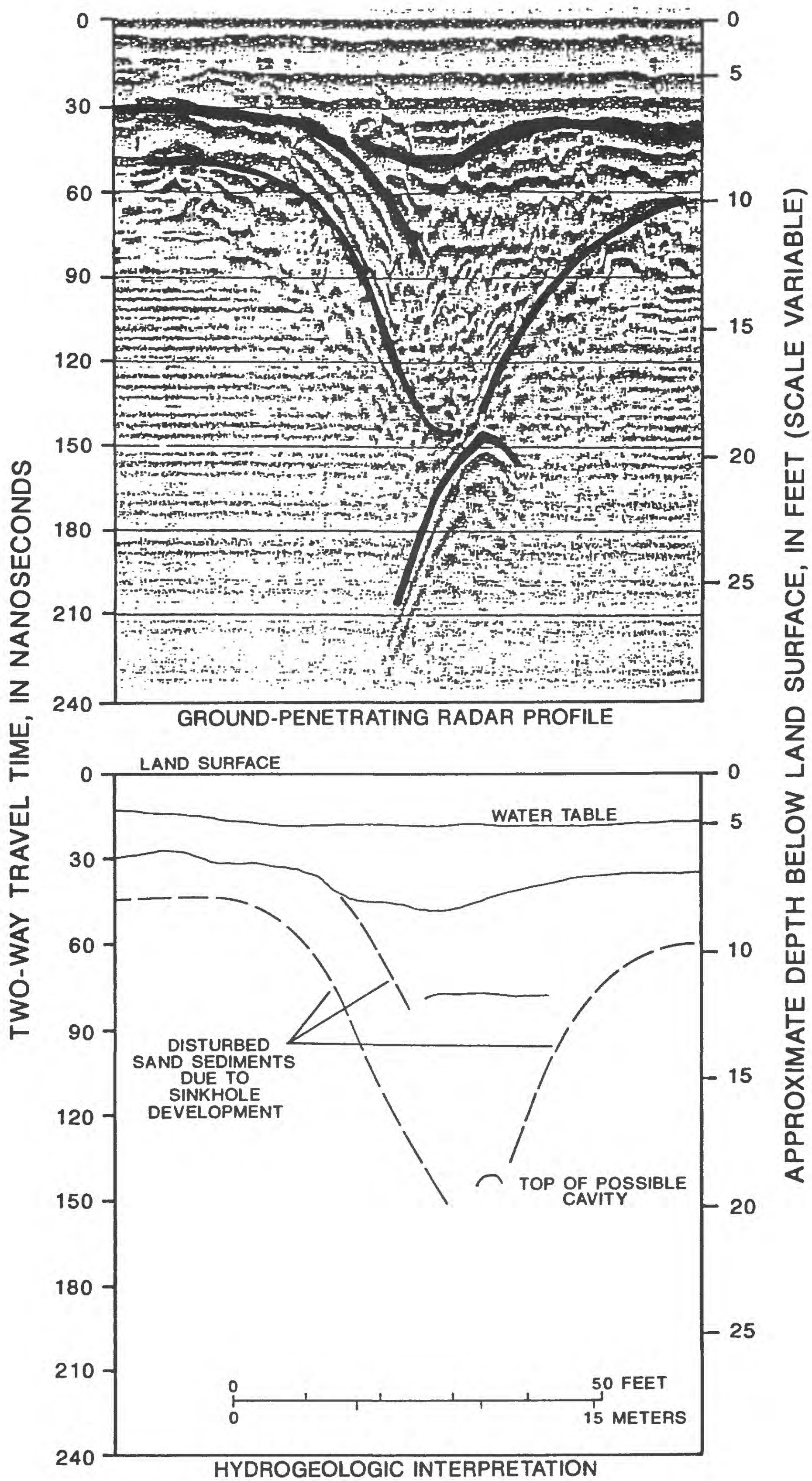

Figure 12. Ground-penetrating radar profile and hydrogeologic interpretation along a traverse over a subsurface cavity at the Pemberton Creek site.

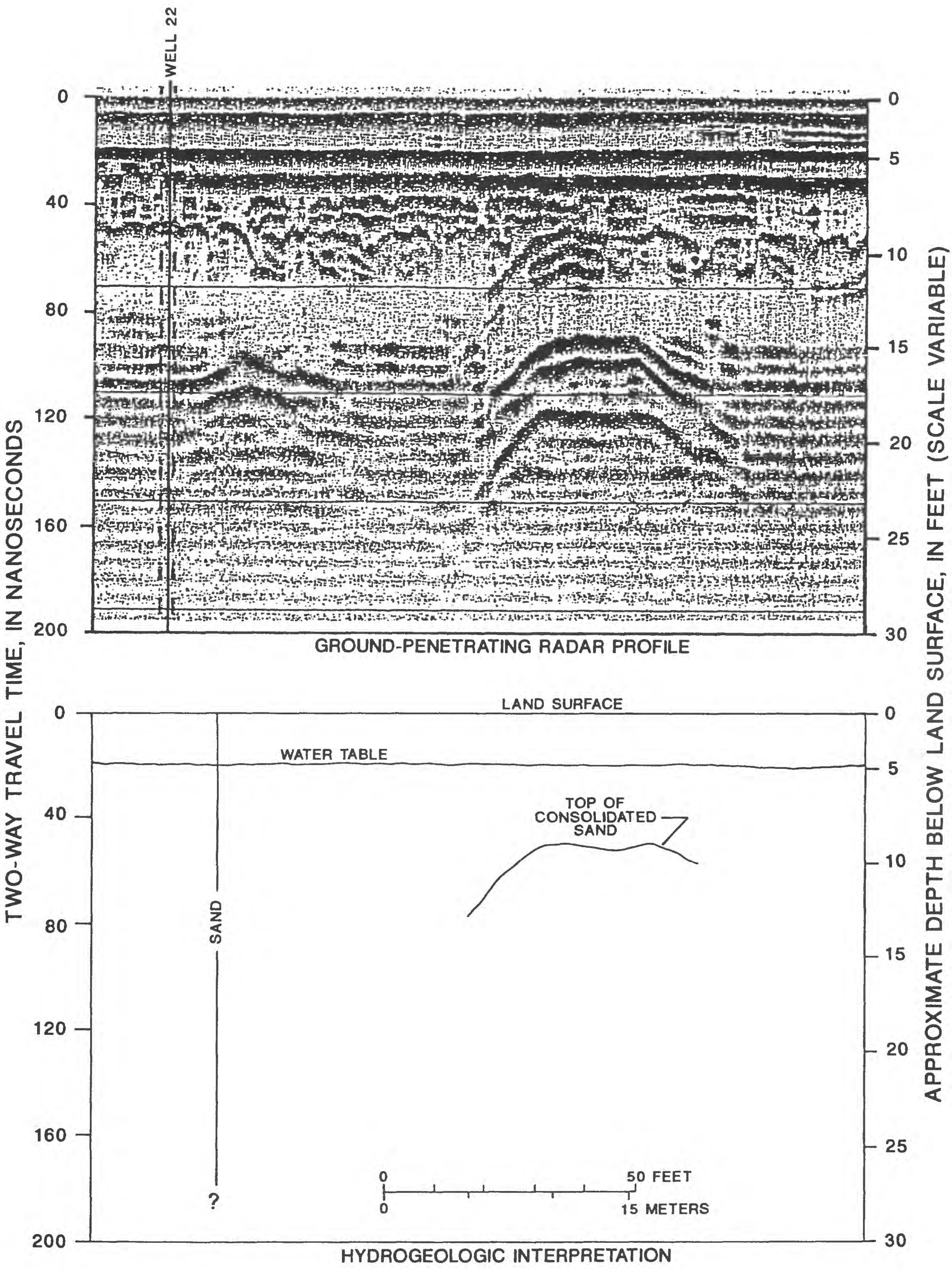

Figure 13. Ground-penetrating radar profile and hydrogeologic interpretation along a traverse over a consolidated sand pinnacle at the Pemberton Creek site.

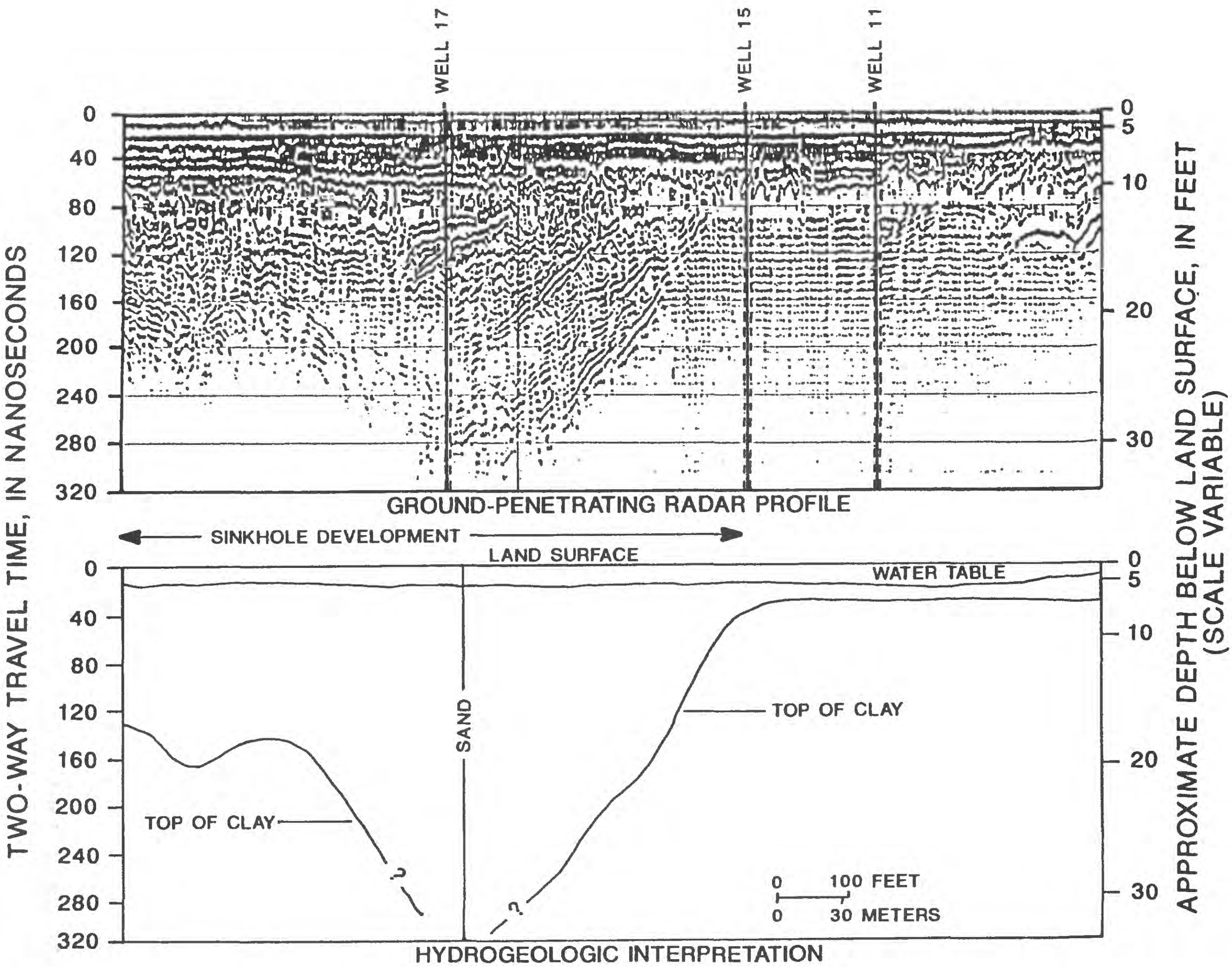

Figure 14. Ground-penetrating radar profile and hydrogeologic interpretation along a traverse over a sinkhole development at the Pemberton Creek site.

A sharp change in reflector direction on the GPR profile may indicate disturbed sediments. Bottom sediments were excavated to deepen a part of a freshwater lake at the Eldridge-Wilde site (fig. 18). The area of the excavation is apparent in the GPR profile as an area where the disturbed sediments settled into flat layers in the deeper parts of the excavation.

Bottom and sediment structures of fresh surface-water bodies can be profiled by GPR because radar energy is attenuated only slightly by freshwater. GPR bottom profiling is precluded in estuaries because the highly conductive seawater greatly attenuates radar energy. Conductive sediments, such as silt and clay, also can restrict subbottom profiling (Haeni and others, 1987).

Hydrogeologic conditions, lithology, and lithologic correlations can be inferred from interpretation of calibrated GPR data. Breaches in confining beds identified on a GPR profile, for example, may indicate potential for ground-water flow between upper and lower aquifers. GPR interpretations can be used for lithologic and hydrogeologic correlations by showing continuity or discontinuity of subsurface features. Interpretations of the GPR profile in figure 9, for example, indicate that the clay layer is continuous between the three wells.

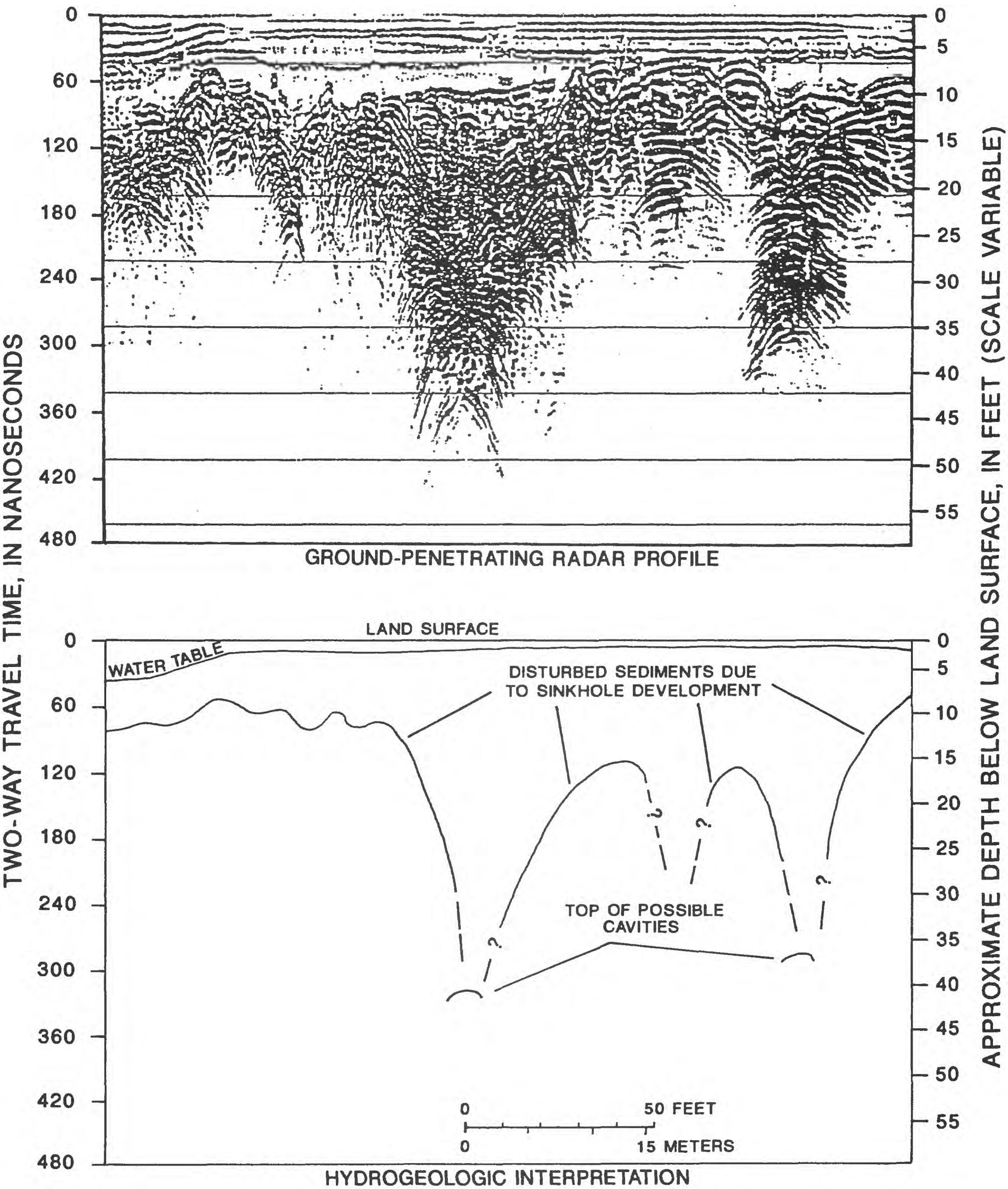

Figure 15. Ground-penetrating radar profile and hydrogeologic interpretation along a traverse over a sinkhole development at the Northwest Pinellas Sewage Treatment Plant site.

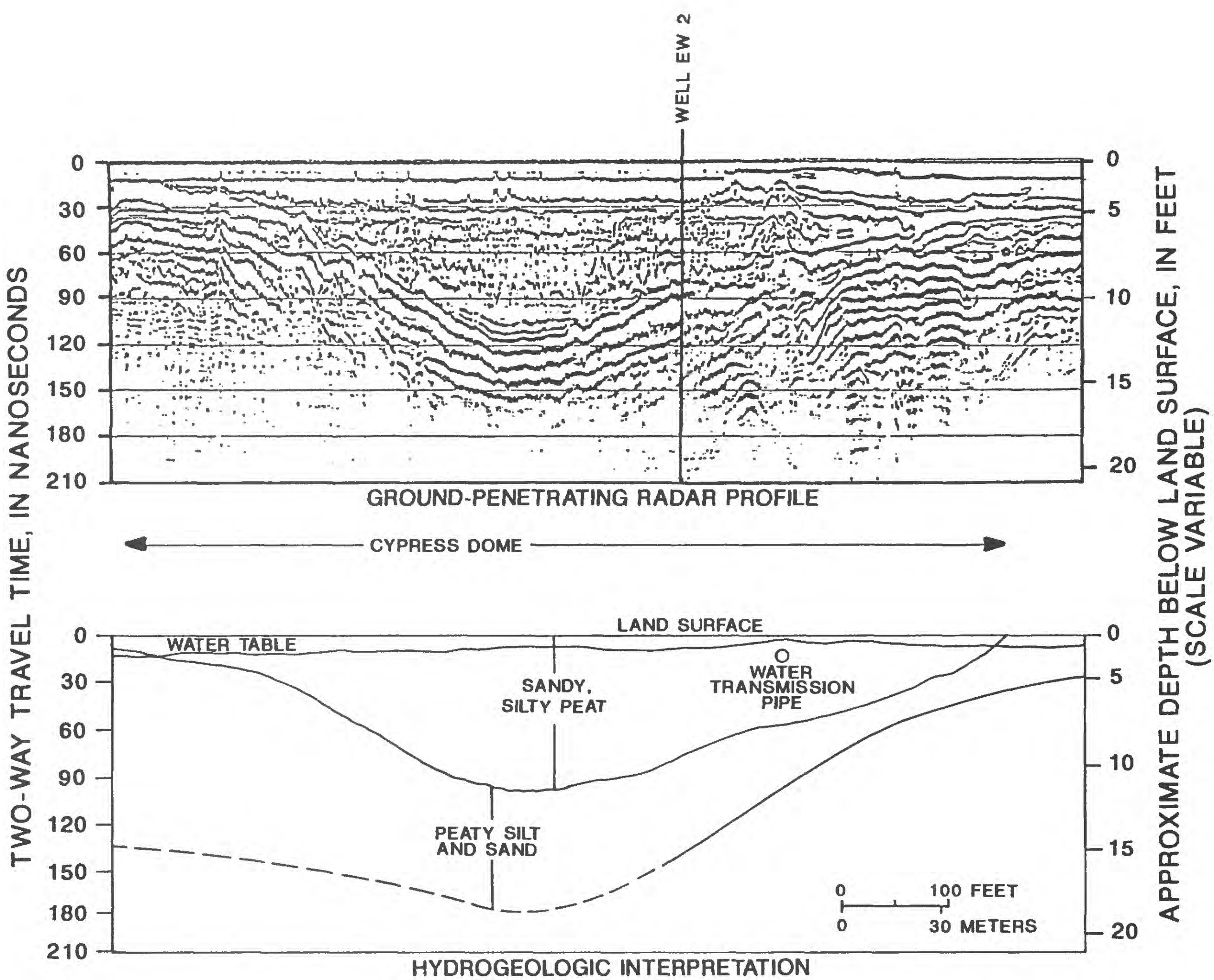

Figure 16. Ground-penetrating radar profile and hydrogeologic interpretation along a traverse over a cypress dome at the Eldridge-Wilde site.

SUMMARY AND CONCLUSIONS

GPR is a relatively inexpensive, nonintrusive, surface geophysical method that can be used to define shallow subsurface lithologic and hydrologic contacts and other features. In GPR surveys, a 10- to 1,000-MHz energy pulse is transmitted into the ground, and energy pulses reflected from subsurface interfaces are graphically recorded on a chart. Depths of exploration and velocities of the energy pulses in the subsurface are principally determined by the electrical properties of the sediment that include pore-fluid properties, conductance, and dielectric constant. In west-central Florida, only shallow exploration depths were possible in areas underlain by clay, whereas greater exploration depths were possible in areas underlain by material composed primarily of sand. Exploration depths from several feet to more than 50 ft were possible in unsaturated and saturated sand and clay sediments in the study areas.

GPR was used in a karst setting in west-central Florida to develop profiles of sediment thickness; to describe depths to the water table and to clay beds; to identify sinkholes, karst development, and buried objects; and to examine lake bottom structure. These GPR profiles were used in conjunction with available hydrologic and lithologic data at selected wells to describe the lithologic and hydrogeologic settings along traverses over several areas. Subsurface deformation features were detected using GPR techniques in areas where surface depressions were observed.

The GPR techniques also were useful in detecting subsurface sediment deformation features indicative of sinkhole development, even in areas where surface depressions were not visible.

The quality of GPR data depends upon the user's knowledge of the equipment, the local hydrogeologic setting, and the ability of the user to interpret the graphic profile. Understanding the GPR data collected at a site and arriving at a correct interpretation of the data may require some other field observations and verification of the subsurface lithology and features. Interpretation of GPR graphic profiles can be simple if sediment stratigraphy is not complex and there are sharp contrasts between subsurface interfaces. If sediment stratigraphy is complex, however, interpretations of GPR profiles can be difficult, although data-processing methods, such as digital signal filtering to remove multiple reflections and other signal conditioning techniques, can be used to aid the interpretation of the GPR data.

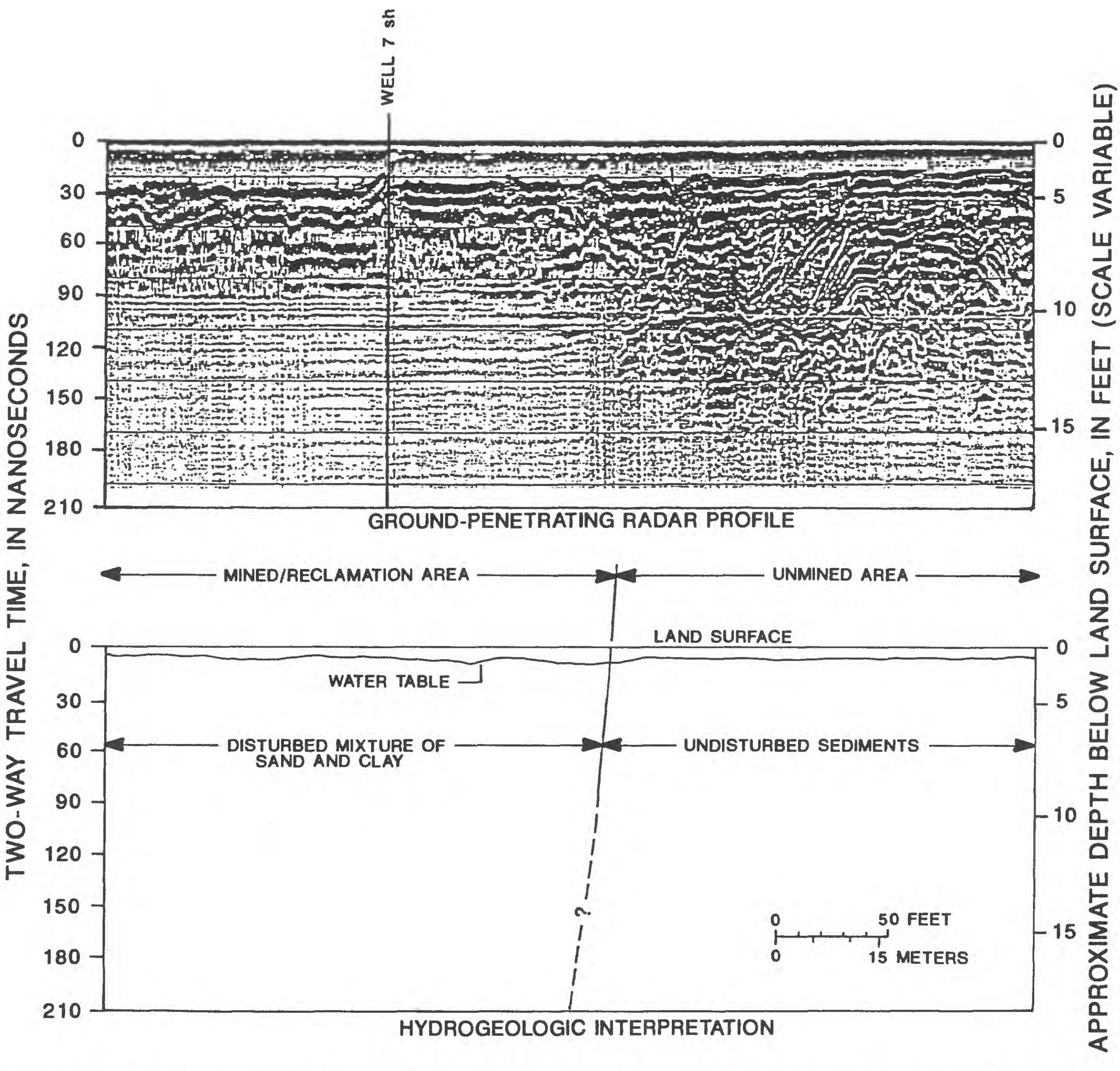

Figure 17. Ground-penetrating radar profile and hydrogeologic interpretation along a traverse over a phosphate mined-reclamation area at the CF Industries site.

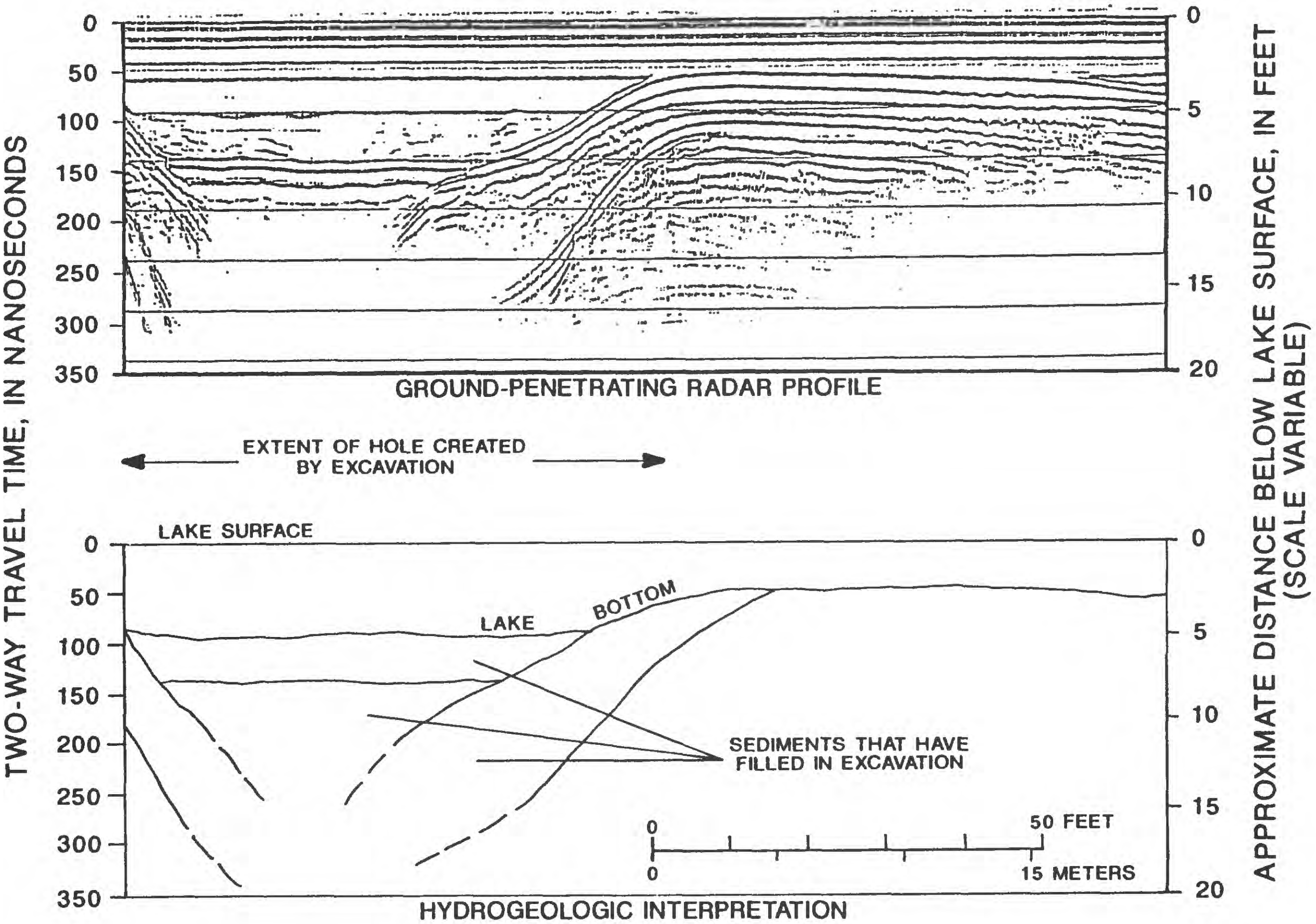

Figure 18. Ground-penetrating radar profile and hydrogeologic interpretation along a traverse over a lake bottom at the Eldridge-Wilde site.

SELECTED REFERENCES

Ballard, R.F., 1983, Electromagnetic (radar) techniques applied to cavity detection: U.S. Army Corps of Engineers Water Way Experiment Station Technical Report-GL-83-1, Report No. 5, 90 p.

Beck, B.F., and Wilson, W.L., 1988, Interpretation of ground-penetrating radar profiles in karst terrane: National Water Well Association Second Conference on Environmental Problems in Karst Terrane and their Solutions, Nashville, Tenn., November 16-18, 1988, Proceedings, p. 347-367.

Benson, R.C., Glaccum, R.A., and Noel, M.R., 1982, Geophysical techniques for sensing buried wastes and waste migration: Prepared by Technos, Inc., Miami, consultants for U.S. Environmental Protection Agency, 331 p.

Beres, M., Jr., and Haeni, F.P., 1991, Application of ground-penetrating radar methods in hydrogeologic studies: Ground Water, v. 29, no. 3, p. 375-386.

Doolittle, J.A., 1988, Ground-penetrating radar (GPR) survey at Tell Halif, Israel: Second International Symposium of Geotechnical Applications of Ground-Penetrating Radar, Gainesville, Fla., March 6-10, 1988, Proceedings, p. 180-213.

Duerr, A.D., Hunn, J.D., Lewelling, B.R., and Trommer, J.T., 1988, Geohydrology and 1985 water withdrawals of the aquifer systems in southwest Florida, with emphasis on the intermediate aquifer system: U.S. Geological Survey Water-Resources Investigations Report 87-4259, 115 p.

Geophysical Survey Systems, Inc., 1974, Continuous subsurface profiling by impulse radar: Hudson, N.H., Geophysical Survey Systems, Inc., 20 p.

———1986, Operation manual SIR system.

Haeni, F.P., McKeegan, D.K., and Capron, D.R., 1987, Ground-penetrating radar study of the thickness and extent of sediments beneath Silver Lake, Berlin, and Meriden, Connecticut: U.S. Geological Survey Water-Resources Investigations Report 85-4108, 19 p.

Miller, J.A., 1986, Hydrogeologic framework of the Floridan aquifer system in west-central Florida and in parts of Georgia, Alabama, and South Carolina: U.S. Geological Survey Professional Paper 1403-B, 91 p., 33 pl.

Morey, R.M., 1974, Continuous subsurface profiling by impulse radar: American Society of Civil Engineers Engineering Foundation Conference on Subsurface Exploration for Underground Excavation and Heavy Construction, Henniker, N.H., August 11-16, 1974, Proceedings, p. 213-232.

National Oceanic and Atmospheric Administration, 1990, Climatological data 1951-80, Florida: Monthly summary, January 1990.

Olson, C.G., and Doolittle, J.A., 1985, Geophysical techniques for reconnaissance investigations of soils and surficial deposits in mountainous terrain: Soil Science Society of America Journal, v. 49, p. 1490-1498.

Ryder, P.D., 1985, Hydrology of the Floridan aquifer system in west-central Florida: U.S. Geological Survey Professional Paper 1403-F, 63 p., 1 pl.

Scott, T.M., 1988, The lithostratigraphy of the Hawthorn Group (Miocene) of Florida: Florida Geological Survey Bulletin 59, 148 p.

Sellmann, P.V., Arcone, S.A., and Delaney, A.J., 1983, Radar profiling of buried reflectors and the ground water table: Hanover, N.H., Cold Regions Research and Engineering Laboratory Report 83-11, 10 p.

Sheriff, R.E., compiler, 1984, Encyclopedic dictionary of exploration geophysics (2d ed.): Tulsa, Okla., Society of Exploration Geophysicists, 323 p.

Southeastern Geological Society, 1986, Hydrologic units of Florida: Florida Bureau of Geology Special Publication 28, 9 p.

Telford, W.M., Geldart, L.P., Sheriff, R.E., and Keys, D.A., 1978, Applied geophysics: London, Cambridge University Press, 860 p.

Ulriksen, C.P.F., 1982, Application of impulse radar to civil engineering: Lund, Sweden, Lund University of Technology, Ph.D. dissertation, 179 p.

U.S. Fish and Wildlife Service, 1985, Wetlands and deepwater habitats of Florida: U.S. Fish and Wildlife Service National Wetlands Inventory, 1 sheet.

*U.S. GOVERNMENT PRINTING OFFICE 1993-733-120/ 80003